# Evaporación oceánica y precipitación

**Luis Gimeno Presa**

**Raquel Nieto Muñiz**

**(Facultad de Ciencias de Ourense. EPhysLab)**

l.gimeno@uvigo.es

rnieto@uvigo.es

# Circulaciones Monzónicas

**Rogert Sorí Gómez**

**(Facultad de Ciencias de Ourense. EPhysLab)**

rogert.sori@uvigo.es

# Prácticas

**Rogert Sorí Gómez**

**(Facultad de Ciencias de Ourense. EPhysLab)**

rogert.sori@uvigo.es

Clases expositivas

*Cuestionario de preguntas (día examen)*

Lecturas de artículos

*Exposición*

Prácticas

*Informe*

# ARTICLES FOR STUDENT WORK

- Comparación de productos de evaporación oceánica y su tendencia Bernal Rodríguez, Cristina
  Chiu, Long S., Chung-Lin Shie, and Si Gao. Oceanic Evaporation: Trends and Variability. INTECH Open Access Publisher, 2012.

- Salinidad oceánica y flujos de agua dulce (E-P) Brieuc, Thomas
  Durack, Paul J., Susan E. Wijffels, and Richard J. Matear. "Ocean salinities reveal strong global water cycle intensification during 1950 to 2000." Science 336.6080 (2012): 455-458.

- Fuentes de humedad oceánica y precipitación Copete Hernández, María Fernanda
  .Gimeno, Luis, et al. "Influence of the intensification of the major oceanic moisture sources on continental precipitation." Geophysical Research Letters 40.7 (2013): 1443-1450.

- Mecanismos de transporte de humedad y precipitaciones extremas Fernández Rial, Samuel
  Gimeno, Luis et al. "Major Mechanisms of Atmospheric Moisture Transport and Their Role in Extreme Precipitation Events." Annual Review of Environment and Resources 41.1 (2016).

- Mecanismos de transporte de humedad: Atmospheric Rivers Lopez Gardoqui, Marina
  Algarra I., R. Nieto, A.M. Ramos, J. Eiras-Barca, R.M. Trigo, L. Gimeno (2020) Significant increase of global anomalous moisture uptake feeding landfalling Atmospheric Rivers, Nature Communications, Vol. 11, 5082 (2020). DOI: https://doi.org/10.1038/s41467-020-18876-w

- Mecanismos de transporte de humedad: Low level jets Marín Pérez, Clara
  Algarra I., J. Eiras-Barca, R. Nieto, L. Gimeno (2019) Global climatology of nocturnal low-level jets and associated moistur sources and sinks, Atmospheric Research, 229, Pages 39-59.

- Variabilidad del monzón índico Mas Llinàs del Torrent, Aina
  Gadgil, S., Rajeevan, M., & Francis, P. A. (2007). Monsoon variability: Links to major oscillations over the equatorial Pacific and Indian oceans. Current Science, 93(2), 182-194.

- Variabilidad del monzón sudamericano Moreno Ferrer, Laura
  Silva, Viviane, and Vernon E. Kousky. 05 The South American Monsoon System: Climatology and Variability. InTech, 2012.

- Variabilidad del monzón africano Pérez Polo, Sara
  Giannini, Alessandra, R. Saravanan, and P. Chang. Oceanic forcing of Sahel rainfall on interannual to interdecadal time scales." Science 302.5647 (2003): 1027-1030

- Monzones en un clima futuro Puentes Jorge, Xabi
  Kitoh, Akio, et al. "Monsoons in a changing world: a regional perspective in a global context." Journal of Geophysical Research: Atmospheres118.8 (2013): 3053-3065.

# Evaporación oceánica y precipitación

**Luis Gimeno Presa**

**Raquel Nieto Muñiz**

**(Facultad de Ciencias de Ourense. Ephyslab)**

l.gimeno@uvigo.es

rnieto@uvigo.es

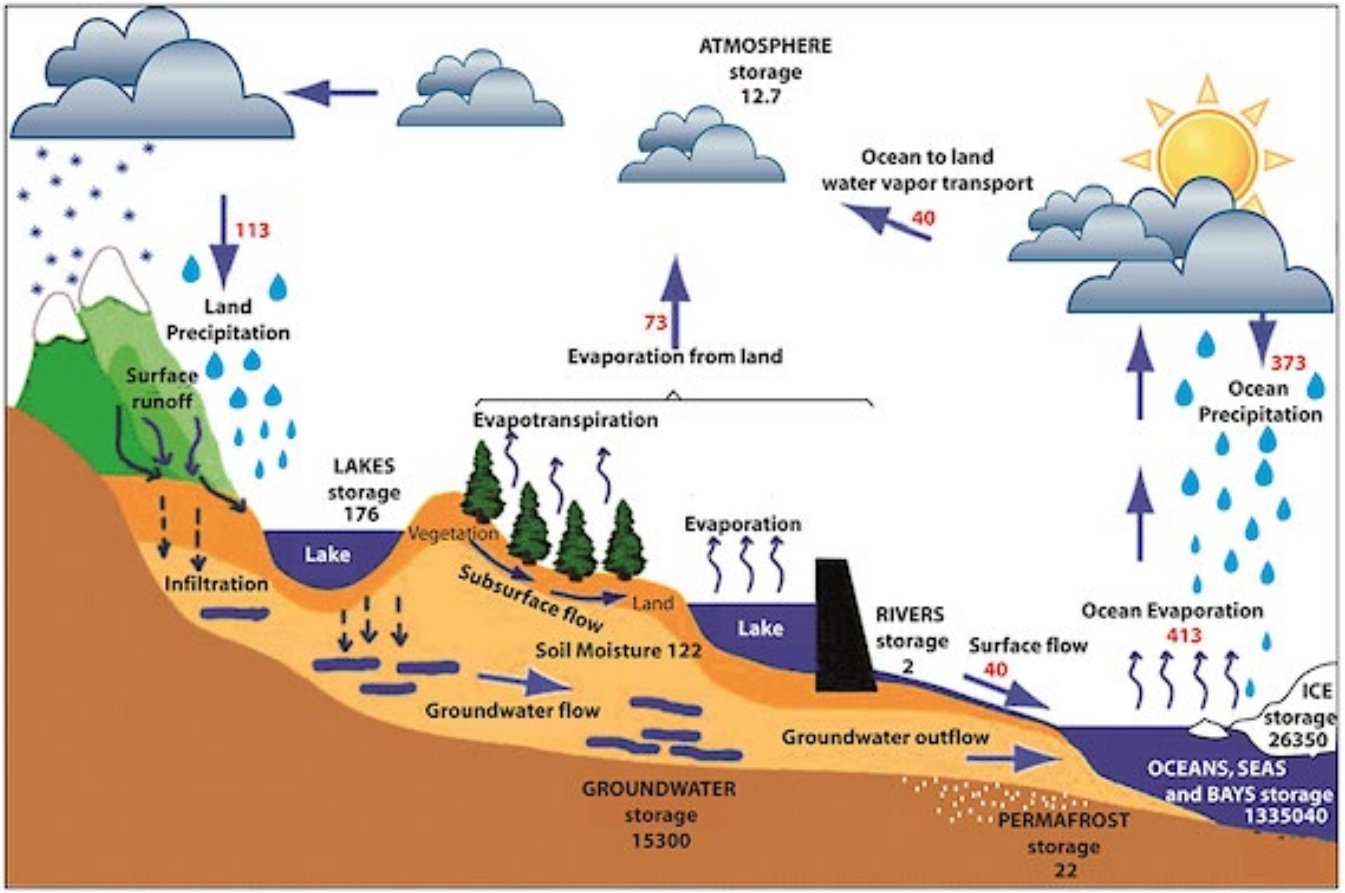


*The hydrological cycle. Estimates of the observed main water reservoirs (black numbers, in 103 km3) and the flow of moisture through the system (red numbers, in 103 km3 yr1).*

- ✓ In global terms, the hydrological cycle is responsible for an annual rate of evaporation of about half a million cubic kilometers of water, around 86% of which is from the oceans, with the remainder having its origin in the continents.
- ✓ Most of the water that evaporates from the oceans (90%) is precipitated back into them.
- ✓ Only 10% falls as precipitation over the continents
- ✓ Of this precipitation, approximately two thirds is recycled over the continents, and only one third runs off directly into the oceans

# GLOBAL DISTRIBUTION OF WATER VAPOR



## Ocean evaporation

$$E = c_e U dq = c_e U (q_s - q_a), \quad (1)$$

*where U is the near-surface wind speed, ce is a turbulent exchange coefficient, qs is the saturation specific humidity at the evaporating surface, and qa is the near-surface atmospheric specific humidity.*

$$E = c_e U dq = c_e U (q_s(\mathrm{SST}) - q_a(T_a, \mathrm{RH})), \quad (2)$$

*where qs is the saturation specific humidity for a given sea surface temperature (SST) and qa is the near surface atmospheric specific humidity*

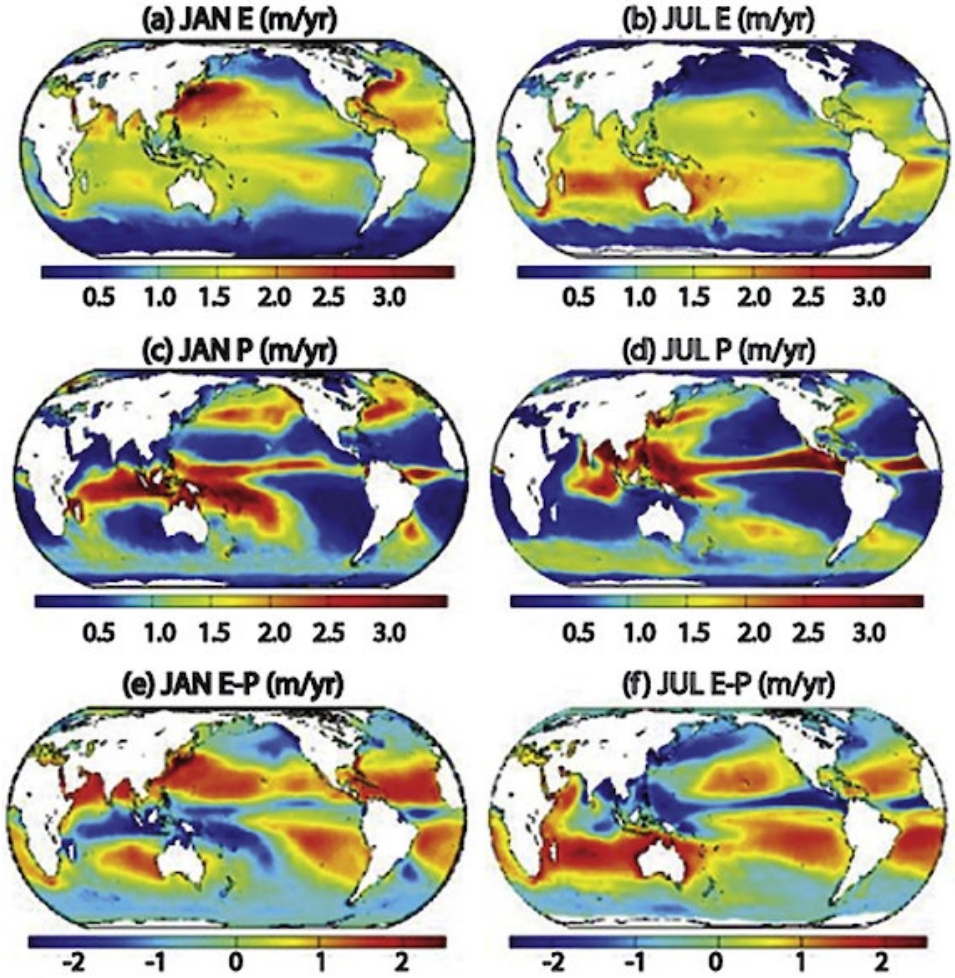


*Ocean time-mean rates of (a, b)E, (c, d) P, and (e, f) E-P for January and July. E is from OAFlux [Yu and Weller, 2007] for 1988–2008, P is from GPCP [Adler et al., 2003] for 1988–2008, and E-P is the combination of these.*

# GLOBAL DISTRIBUTION OF WATER VAPOR



- ✓ Once evaporated, water vapor molecules typically spend about 10 days in the atmosphere before condensing and falling to the Earth as precipitation [Numaguti, 1999]. The 10 day period considered is a median of a broad probability density function of residence times of water vapor in the atmosphere.

- ✓ The climatological mean distribution of global precipitation rate, P, is shown in Slide 3 for January and July using the precipitation data set from the Global Precipitation Climatology Project (GPCP)

- ✓ A combination of satellite-derived E and P data sets yields estimates of global ocean freshwater flux.

- ✓ The balance of E and P indicates the major sources and sinks of water vapor over the globe. The major net sources (E > P) are located over the subtropical belts of high evaporation, and the major net sinks (E < P) are found in the Intertropical Convergence Zone (ITCZ), the South Pacific Convergence Zone (SPCZ), and the midlatitude storm tracks where the convection of moisture results in high precipitation.

# GLOBAL DISTRIBUTION OF WATER VAPOR



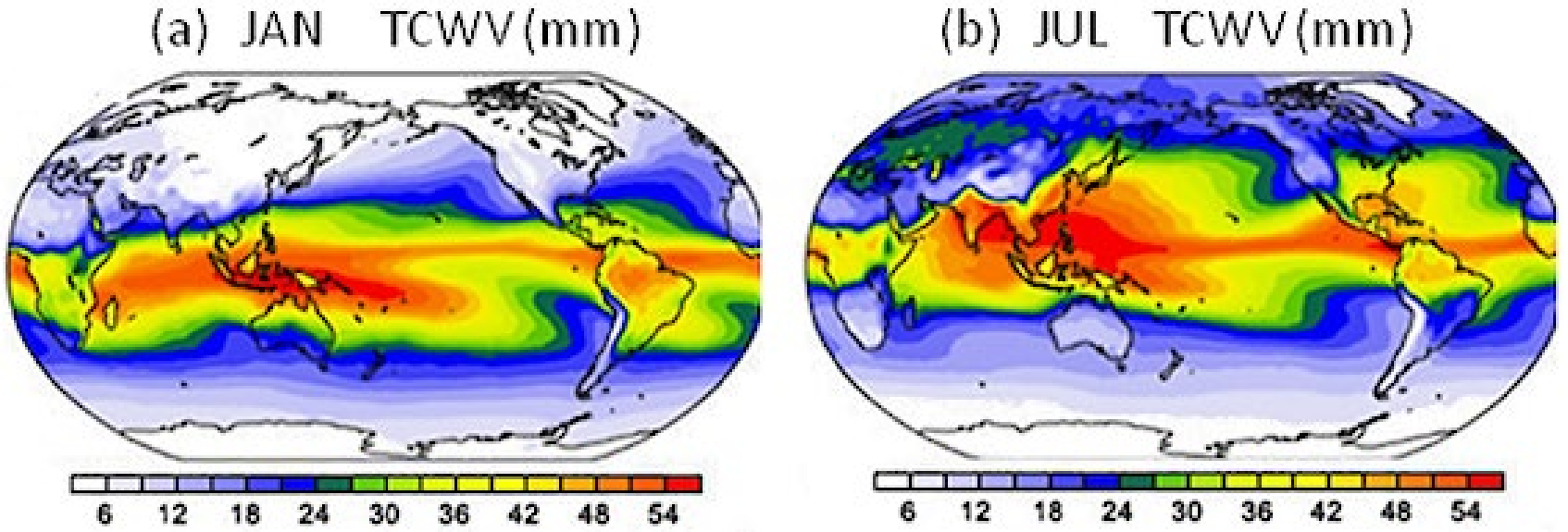


*Mean total column water vapor (TCWV) for (a) January and (b) July.*

- ✓ The overall patterns and temporal variation of water vapor over the oceans generally follow those of SST, because according to the Clausius-Clapeyron (C-C) equation.
- ✓ Because of its sensitivity to temperature, the water vapor content is high in the lower atmosphere, and decreases with height. Moreover, water vapor occurs at high concentrations in the tropics and is less prevalent at higher latitudes.
- ✓ If the total water vapor content in the atmosphere were to condense and precipitate, the depth of precipitation would be about 50 mm at equatorial latitudes, but only about 5 mm at the poles
- ✓ The highest TCWV occurs over the tropical Pacific warm pool

# GLOBAL DISTRIBUTION OF WATER VAPOR

Water Vapor Flux and Divergence

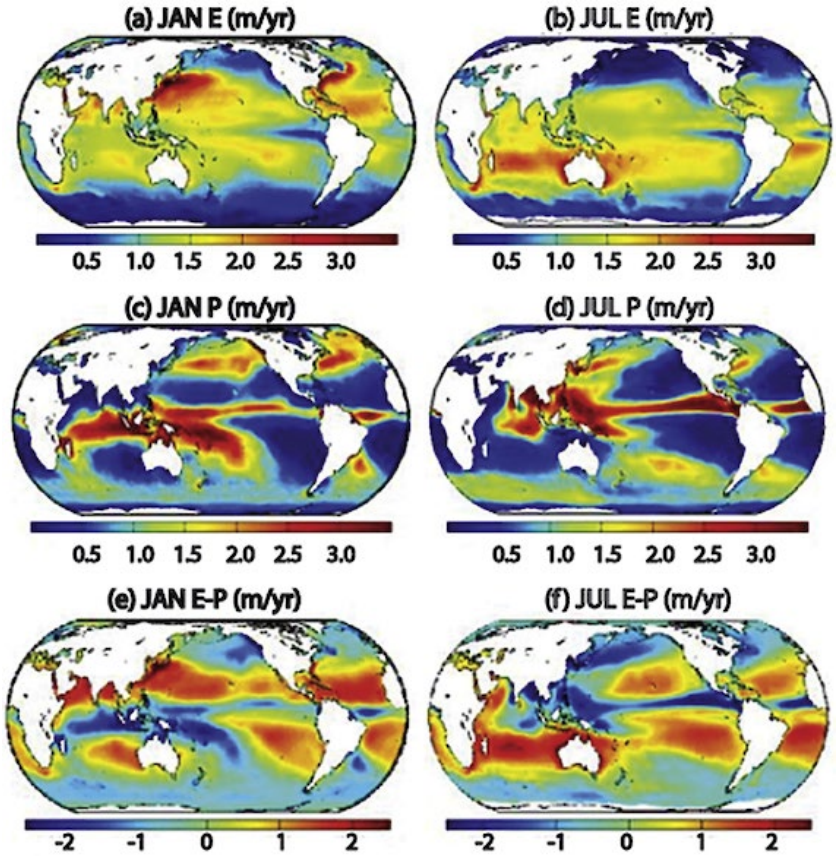


*Ocean time-mean rates of (a, b)E, (c, d) P, and (e, f) E-P for January and July. E is from OAFlux [Yu and Weller, 2007] for 1988–2008, P is from GPCP [Adler et al., 2003] for 1988–2008, and E-P is the combination of these.*

- ✓ The global distribution of evaporation differs from that of atmospheric water vapor and also from that of precipitation This is because for precipitation to occur, three factors are important, namely (1) the availability of atmospheric moisture, (2) a cooling mechanism, and (3) the presence of cloud condensation nuclei (CCN).

- ✓ The global distribution of precipitation is more similar to the distribution of TCWV, particularly in the tropics, in areas of low-level convergence and high SST. In the tropics, there is also far more structure to the patterns of rainfall, due to the effects of major circulation regimes such as the monsoons and the Hadley

The transport of water vapor in the atmosphere is typically represented by the vertically integrated total horizontal flux of water vapor, which can be expressed as

$$\Theta = \frac{1}{g}\int_0^{p_s} q\mathbf{V}dp, \qquad (5)$$

where g is the acceleration due to gravity, p is the pressure, ps is the pressure at the surface, q is the specific humidity, and V is the horizontal wind vector at a given level, composed of both mean and eddy components. Using the conservation of mass, the hydrological balance in the atmosphere can be formulated as follows:

$$\frac{\partial W}{\partial t} + \nabla \cdot \Theta = E - P, \qquad (6)$$

Equation (6) states that the temporal rate of change of precipitable water, $W = \frac{1}{g}\int_0^{p_s} qdp$ and the divergence of the water vapor transport integrated over the depth of the atmosphere $(\nabla \cdot \Theta)$ must balance the fresh water flux E-P at the surface.

# GLOBAL DISTRIBUTION OF WATER VAPOR

Water Vapor Flux and Divergence

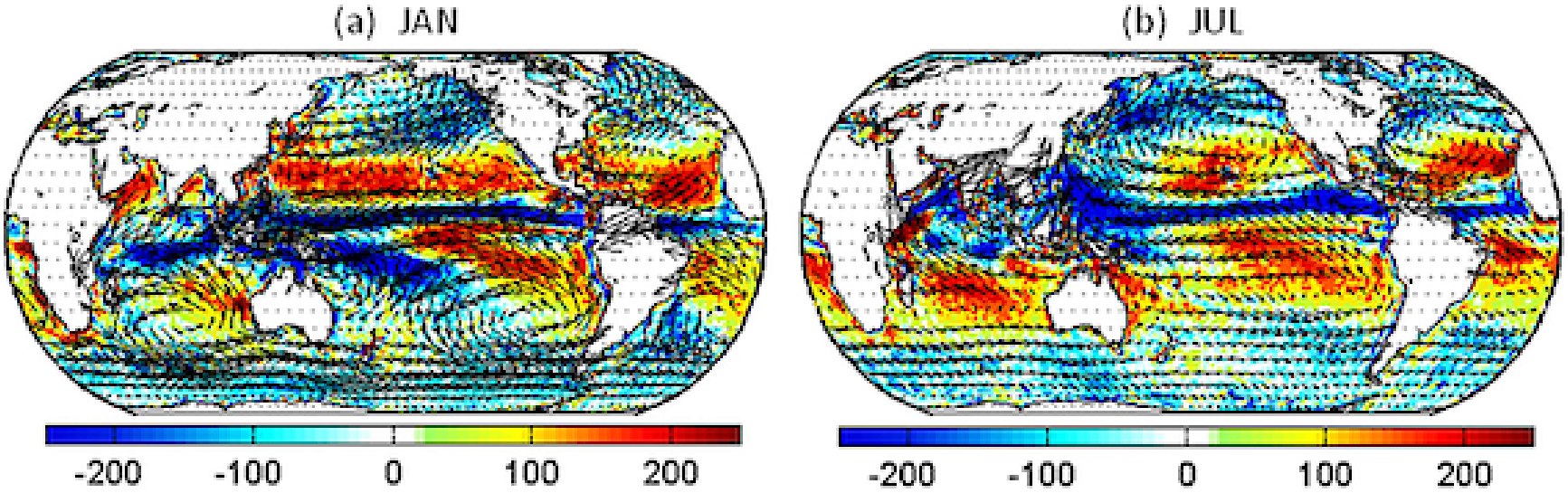


*Vector field of the vertically integrated total horizontal flux of water vapor Θ (unit: kg/m/s) superimposed on the flux divergence (∇ · Θ; unit: cm/yr) for (a) January and (b) July.*

- ✓ There is a good agreement between the geographical distributions of $\nabla \cdot \Theta$ in Figures above and E-P in previous slides, demonstrating that, averaged over time, the rate of change of water storage is small, and E-P is largely balanced by $\nabla \cdot \Theta$

- ✓ Throughout the year, the transport of water vapor in the tropics is characterized by a broad band of easterly transport in the Atlantic Ocean and the central and eastern Pacific and by a seasonal reversal of direction in the Indian Ocean and its vicinity, in association with monsoons .Outside the tropics, water vapor is transported poleward.

# GLOBAL DISTRIBUTION OF WATER VAPOR



- ✓ The strong easterly fluxes of moisture in the tropics are due to the highest global values of precipitable water. Almost equally strong fluxes occur around the major subtropical anticyclones in the summer hemisphere, and year-round strong westerly and northwesterly fluxes are found in the midlatitude stormtrack. However, while the tropical and subtropical fluxes are quasipermanent in nature, with relatively little daily variation, the averaging masks strong daily variability at the midlatitudes.

- ✓ At any time, there are typically three to five major conduits in each hemisphere, each of which transports large amounts of water vapor in narrow streams from the tropics to the higher latitudes. Newell et al. [1992] termed these conduits “atmospheric rivers” (ARs), because they transport water at volumetric flow rates similar to those of the world’s largest rivers. These structures account for most of the long distance transport of water vapor and contain 95% of the meridional flux of water vapor at latitude 35º

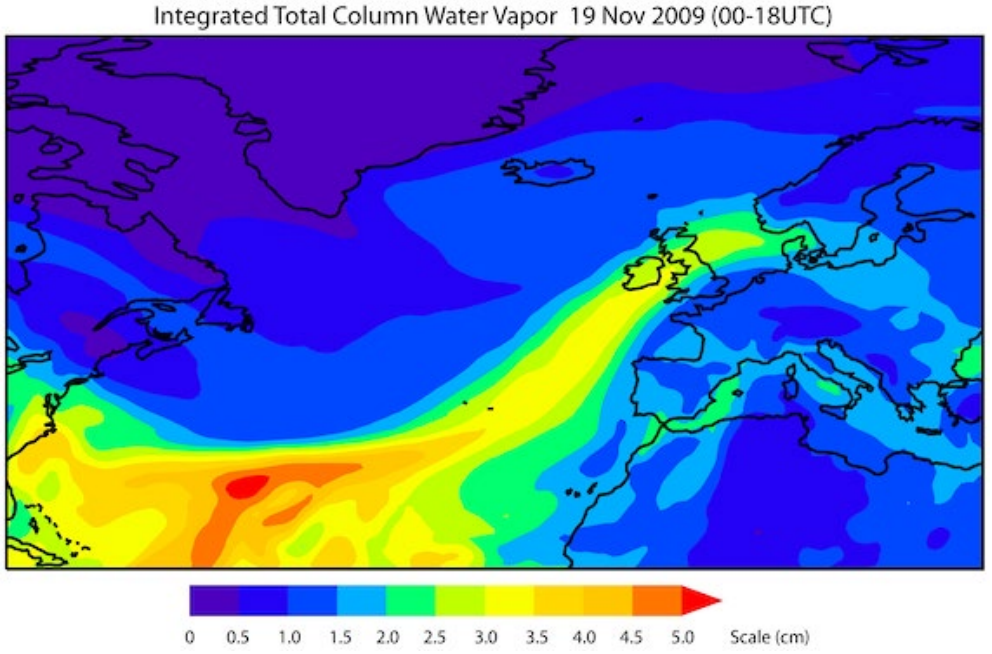


*Daily integrated total column of water vapor showing the AR that affected the UK on 19 November 2009. Data: ERA-Interim.*

# GLOBAL DISTRIBUTION OF WATER VAPOR

Limitations of Available Data Sets

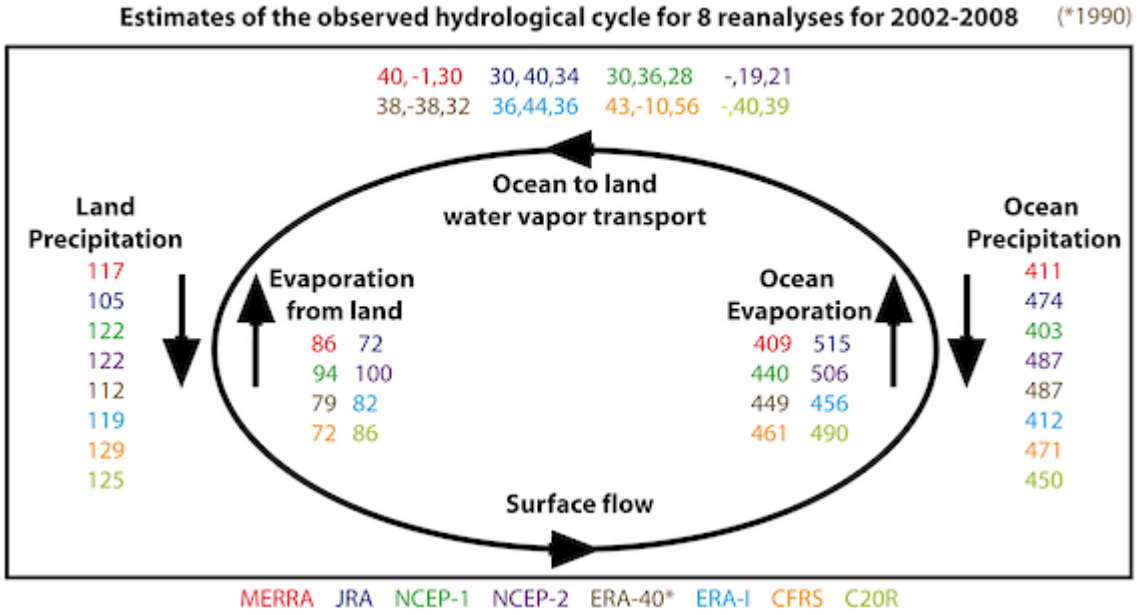


*Estimated values of the observed hydrological cycle using eight reanalyses for 2002–2008, with the exception for ERA-40, which starts from 1990 (color coded as given at the bottom of the figure). For the ocean-to-land water vapor transport, the three estimates given for each are (1) the actual transport estimated from the moisture budget (based on analyzed winds and moisture), (2)E-P from the ocean, and (3) P-E from the land, which should be identical. Units: 1000 km3 yr−1*

- ✓ Although the reanalyses produce quite good results for precipitation over land, over the ocean E, P, and E-P based on model output are not stable. The poorer representation of coastlines and orography may be a source of uncertainty in low-resolution reanalyses.
- ✓ Most reanalysis models, with the exception of MERRA, predict water cycling (P and E) that is too intense over the ocean, although ocean-to-land transports are very close to their observed values
- ✓ All P ocean estimates are high relative to the estimate of GPCP.
- ✓ Apart from MERRA, E ocean estimates from reanalyses are also high when compared with the reference values used herein.

## Analytical or Box Models

All analytical models can be derived from the equation of the vertically integrated balance of water vapor

$$\frac{\partial(w)}{\partial t} + \frac{\partial(wu)}{\partial x} + \frac{\partial(wv)}{\partial y} = E - P, \qquad (7)$$

where w is the amount of water vapor contained in a column of air of unit base area, u is the vertically integrated zonal water vapor flux divided by w (this is equivalent to a water vapor-weighted zonal wind), v is the water vapor weighted meridional wind, E is evaporation, and P is precipitation.

Budyko [1974] developed a model by assuming the following:

(1) a negligible change in storage of atmospheric water,
(2) a one-dimensional (1-D) estimation of recycling, and
(3) a well-mixed atmosphere.

Considering the basic equation of the conservation of mass, assumptions (1) and (2) imply that the first and third terms in equation (7) may be neglected. This is then a simple 1-D estimate of the recycling that takes place within a region

## Analytical or Box Models

After Budyko's initial conceptualization, a number of authors have developed models to expand and improve the quantification of precipitation recycling. The initial 1-D approach was later extended to two dimensions

Dominguez et al. [2006] later developed the "Dynamic Recycling Model (DRM)" in which the assumption of negligible moisture storage was relaxed, and the model could then be used at timescales shorter than a month. In the DRM, equation (7) is solved in a Lagrangian framework, and the local recycling ratio R (the amount of precipitation for a particular cell that originates as evapotranspiration within the selected region) is

$$R = 1 - \exp\left[-\int_0^{\tau} \frac{E}{W} d\tau'\right], \qquad (8)$$

where E is evapotranspiration and W is precipitable water, calculated at different times t, following the trajectory of the parcel. When applied to monthly timescales, the DRM estimates very similar spatial and temporal variability of recycling to the Brubaker et al. [1993] and Eltahir and Bras [1996] models, but the estimates are slightly higher.

## Numerical Water Vapor Tracers

- ✓ This method makes use of numerical water vapor “tagged” tracers (WVT), which is also known as a water vapor “tagging” approach.
- ✓ We can divide these methods into Eulerian and Lagrangian. In the Lagrangian frame of reference the observer follows an individual fluid parcel as it moves through space and time. On the other hand, the Eulerian frame of reference focuses on specific locations in the space through which the fluid flows as time passes.

- ✓ Eulerian tagging techniques not only yield information on recycled precipitation but also account for the specific origin and destination of advected moisture.
- ✓ Numerical tracers are implemented in GCMs and experience the same processes as atmospheric water.
- ✓ Because they are embedded in climate models, numerical WVT models incorporate state-of-the-art understanding of how moisture moves and is transformed as it passes through the atmosphere

The prognostic equation for any given water vapor tracer follows:

$$\frac{\partial q_T}{\partial t} = -\Delta_3 \cdot (q_T V) + \left.\frac{\partial q_T}{\partial t}\right|_{turb} + (E_{surf})_T + f_c \left.\frac{\partial q_T}{\partial t}\right|_{cond} + f_R \left.\frac{\partial q_T}{\partial t}\right|_{revap} + f_{RAS} \left.\frac{\partial q_T}{\partial t}\right|_{RAS}, \quad (9)$$

## Numerical Water Vapor Tracers

During recent years, the use of Lagrangian methods has become popular for diagnosing the transport of moisture and, in particular, for determining the origin of moisture that precipitates in particular regions.

Stohl and James [2004, 2005] developed an analog method that accounts for the net loss and/or gain of moisture along trajectories using:

$$(e-p)_k = m\frac{dq}{dt}, \qquad (12)$$

where (e-p)k are the rates of increase and decrease of moisture along the trajectory of each particle and (q) is the specific humidity taken from the meteorological (e.g., reanalysis) data, which are also used as input to the Lagrangian model. By filling the atmosphere with a large number of computational air particles, the surface freshwater flux in an area A can be determined using

$$E-P = \frac{\sum_{k=1}^{K}(e-p)_k}{A}, \qquad (13)$$

where a budget is calculated for all K particles that reside above A. Thus, the surface freshwater flux E-P can be accounted for, using information on the trajectories of the particles. Net loss or gain of moisture can be identified both along individual particle trajectories as well as on a regular grid, using only particle information. With this methodology, the evaporative source and sink regions for a given area can be identified and linked using the trajectory information.

# SOURCES AND SINKS OF ATMOSPHERIC MOISTURE

Methods Used to Establish Source Receptor Relationships

## Physical Water Vapor Tracers

- ✓ Although analytical and numerical models are powerful tools for studying atmospheric recycling, they must be validated using physical measurements.
- ✓ The heavy stable isotopes of hydrogen and oxygen, D (deuterium) and 18O in precipitation and/or water vapor, are ideal measurable parameters because they are an integrated product of both the history of an air mass and the specific prevailing meteorological conditions (temperature as well as humidity and wind speed) at the time of condensation
- ✓ Because of differences in mass, mixtures of H216O/HD16O and H216O/H218O have different chemical and physical properties.
- ✓ Therefore, when the water changes phase, the heavy isotopes (HD16O and H218O) become preferentially enriched in the liquid rather than the gas phase and in the solid rather than the liquid phase. This is called isotopic fractionation.
- ✓ Phase changes always occur during the circulation of atmospheric water, and geographical and temporal differences in isotopic ratios therefore emerge in vapor and precipitation.

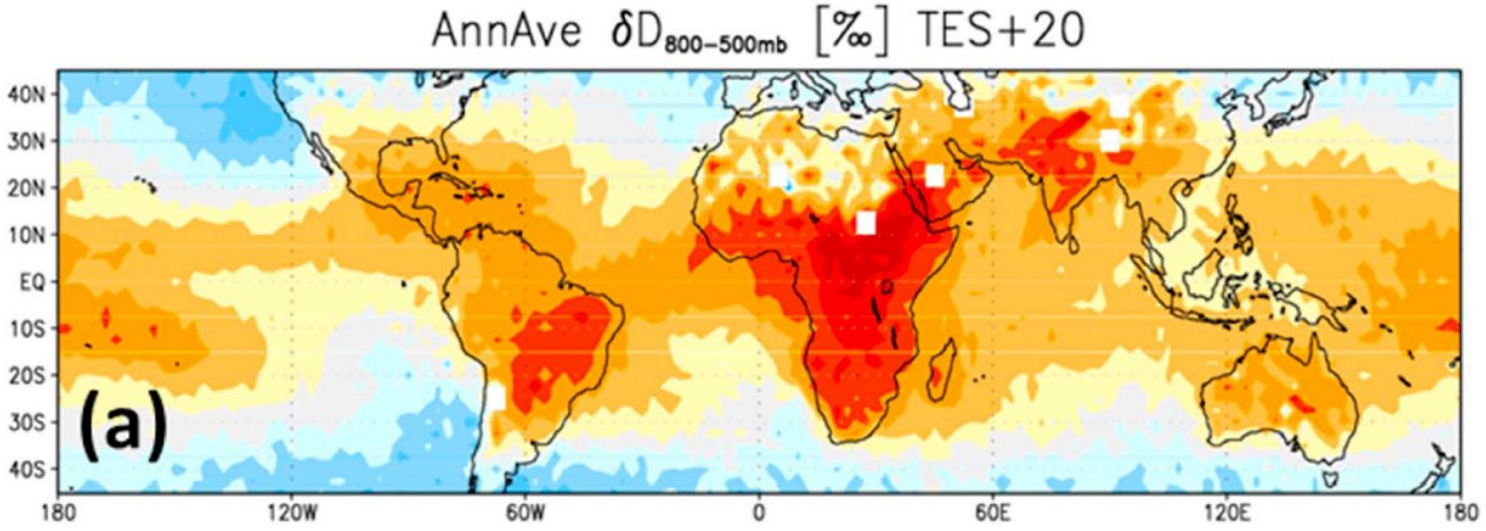


*Mean climatology of δD in midtropospheric water vapor (800 to 500 hPa pressure) for TES*

## Summary of the Main Strengths and Weaknesses of Analytical Box Models and Physical and Numerical (Eulerian and Lagrangian) Water Vapor Tracer Method

| Type | Strength | | Weakness |
|---|---|---|---|
| Analytical Box Models | Simple as few parameters are required and they consider grid based spatial variability. | | Neglects in-boundary processes; some are based on the well mixed assumption (the local source of water is well mixed with all other sources of water in the whole vertical column); most are only valid for monthly or longer timescales. |
| Physical Water Vapor Tracers | Simplicity; global coverage; include vertical processes; reanalysis input data (high spatiotemporal resolution); enable the combination of GCMs and Lagrangian Rayleigh models. | | Sensitivity of the isotopic signal; calculation time; availability of data for validation; does not account for convection and rainwater evaporation/equilibration. |
| Numerical Water Vapor Tracers | Eulerian | Detailed atmospheric processes; realistic moisture circulation. | Dependent on the model bias; global forcing is required; poor representation of short-timescale hydrological cycle parameters; does not include the remote sources of water for a region. |
| | Lagrangian | High spatial resolution moisture sources diagnostics; quantitative interpretation of moisture origin allowed; not limited by a specific RCM domain and spin-up; net freshwater flux can be tracked from a region both forward and back ward in time; realistic tracks of air parcels; computationally efficient | Sensitivity of moisture flux computations to increases in data noise for shorter time periods or smaller regions; surface fluxes under (over) estimation if dry (cold) air masses tracking as the budget is not closed; evaporation rates are based on calculations rather than observations in some methods; evaporation and precipitation are not clearly |

# SOURCES AND SINKS OF ATMOSPHERIC MOISTURE

## Intercomparison of the Source-Receptor Methods

An Example for the Iberian Peninsula

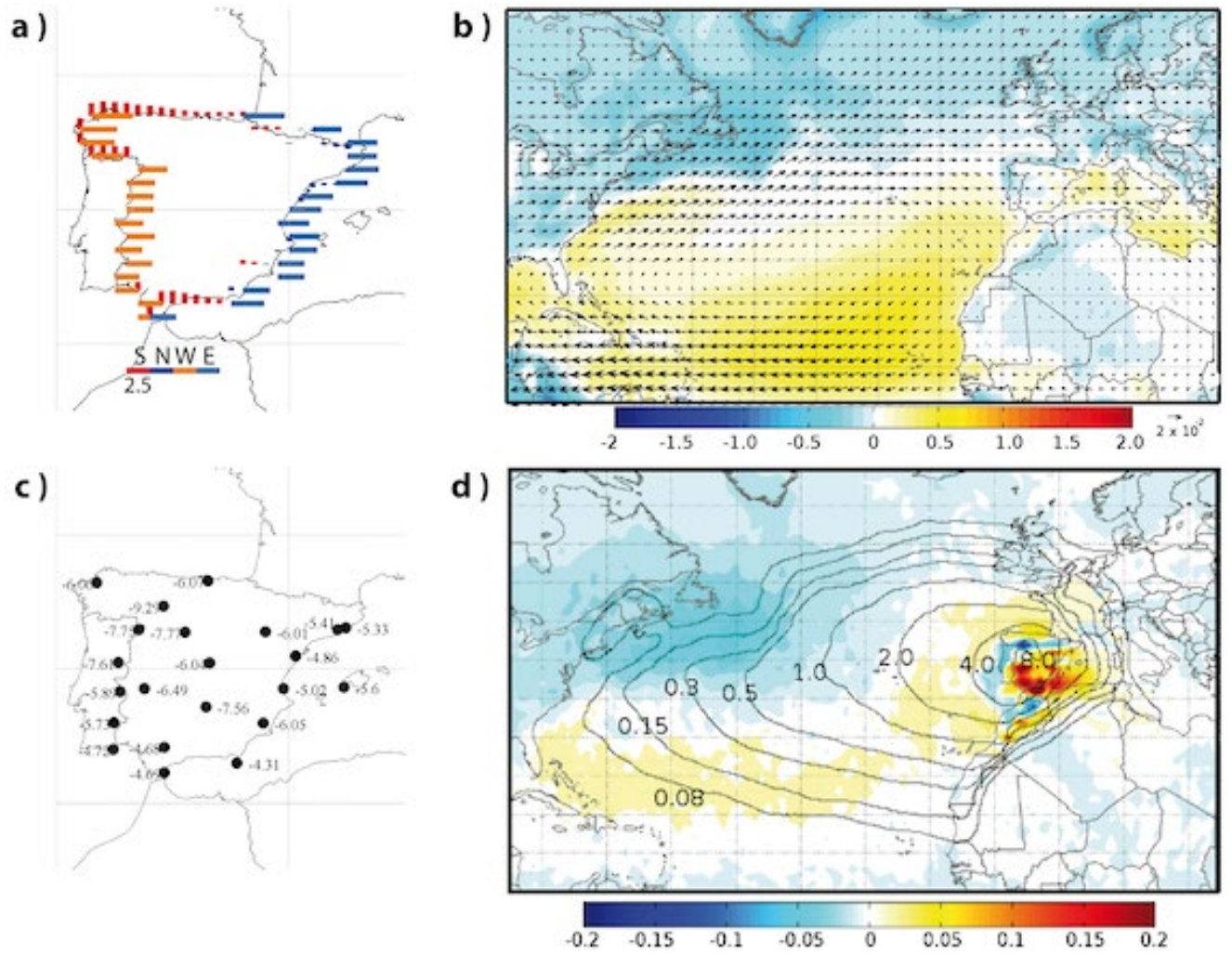


*Comparison among the results obtained using different methods for the climatological mean pattern for 2000–2004 for Spain: (a) simple box model showing the moisture flux across the segments of zonal and meridional regional boundaries; (b) typical Eulerian field method using vertically integrated water vapor flux (shaded) and moisture flux vectors (black arrows); (c) long-term weighted delta18O in precipitation in the GNIP stations; (d) identification of the sources of moisture using ten-day integrated net freshwater flux from FLEXPART backward trajectories (shaded contours) and from quasi-isentropic back trajectory analysis of atmospheric water vapor (solid lines)*

# SOURCES AND SINKS OF ATMOSPHERIC MOISTURE

## Global Source and Sink Regions of Moisture

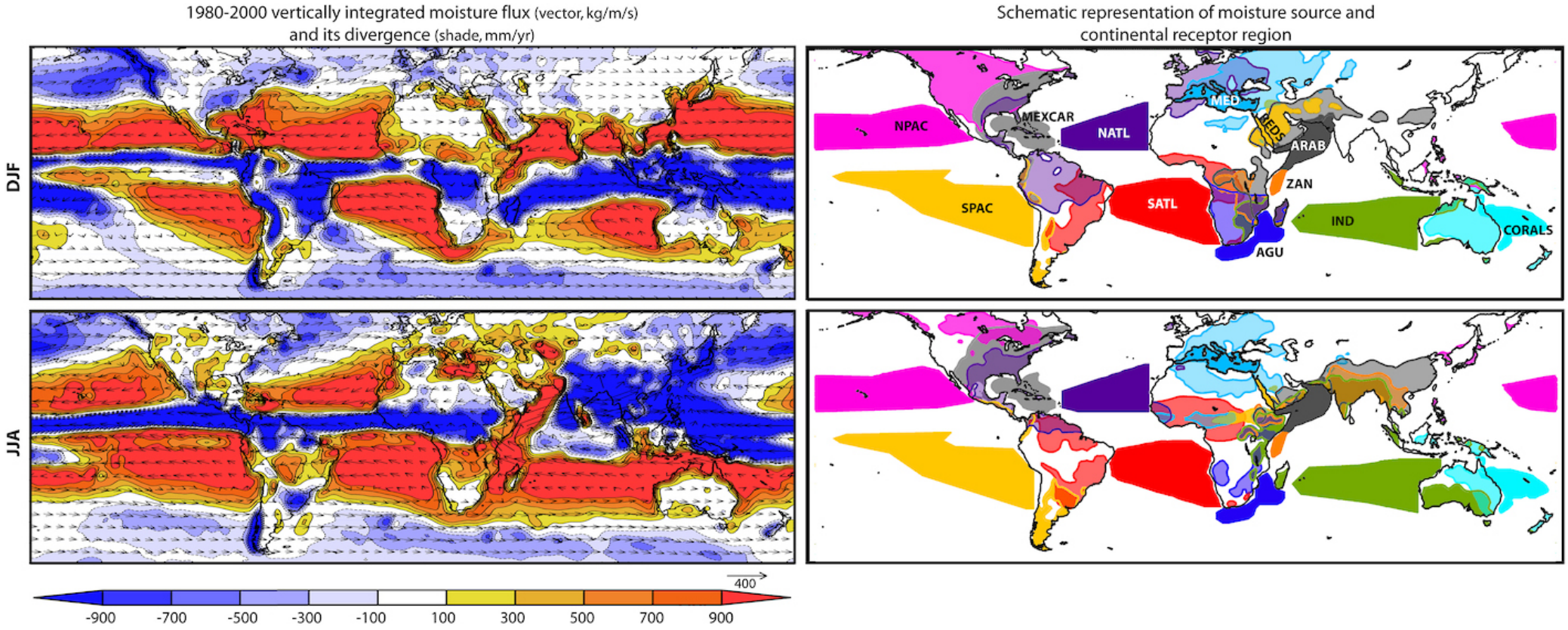


*(left) The 1980–2000 vertically integrated moisture flux (vector; kg m−1 s−1) and its divergence (contours; mm yr−1) for JJA and DJF.. (right) Schematic representation of moisture source and continental receptor regions for the period 1980–2000 for JJA and DJF. The sources of moisture (indicated in the bottom right panel) are as follows: NPAC, North Pacific; SPAC, South Pacific; NATL, North Atlantic; SATL, South Atlantic; MEXCAR, Mexico Caribbean; MED, Mediterranean Sea; REDS, Red Sea; ARAB, Arabian Sea; ZAN, Zanzibar Current; AGU, Agulhas Current; IND, Indian Ocean; CORALS, Coral Sea (as in Gimeno et al. [2010a]). Six of these source regions were defined using the threshold of 750 mm yr−1 of the annual vertically integrated moisture flux calculated for the period 1958–2001 using data from ERA40 for the oceanic sources. The Mediterranean Sea and the Red Sea were defined using their physical boundaries [from Gimeno et al., 2010a]. Only negative values of E-P larger than −0.05 mm d−1 are plotted over the continents and are shown in the same colors as the corresponding oceanic source region. Overlapping continental regions are plotted with the appropriate shading mask. E-P fields are calculated by forward tracking from the moisture sources defined.*

# SOURCES AND SINKS OF ATMOSPHERIC MOISTURE

## Global Source and Sink Regions of Moisture

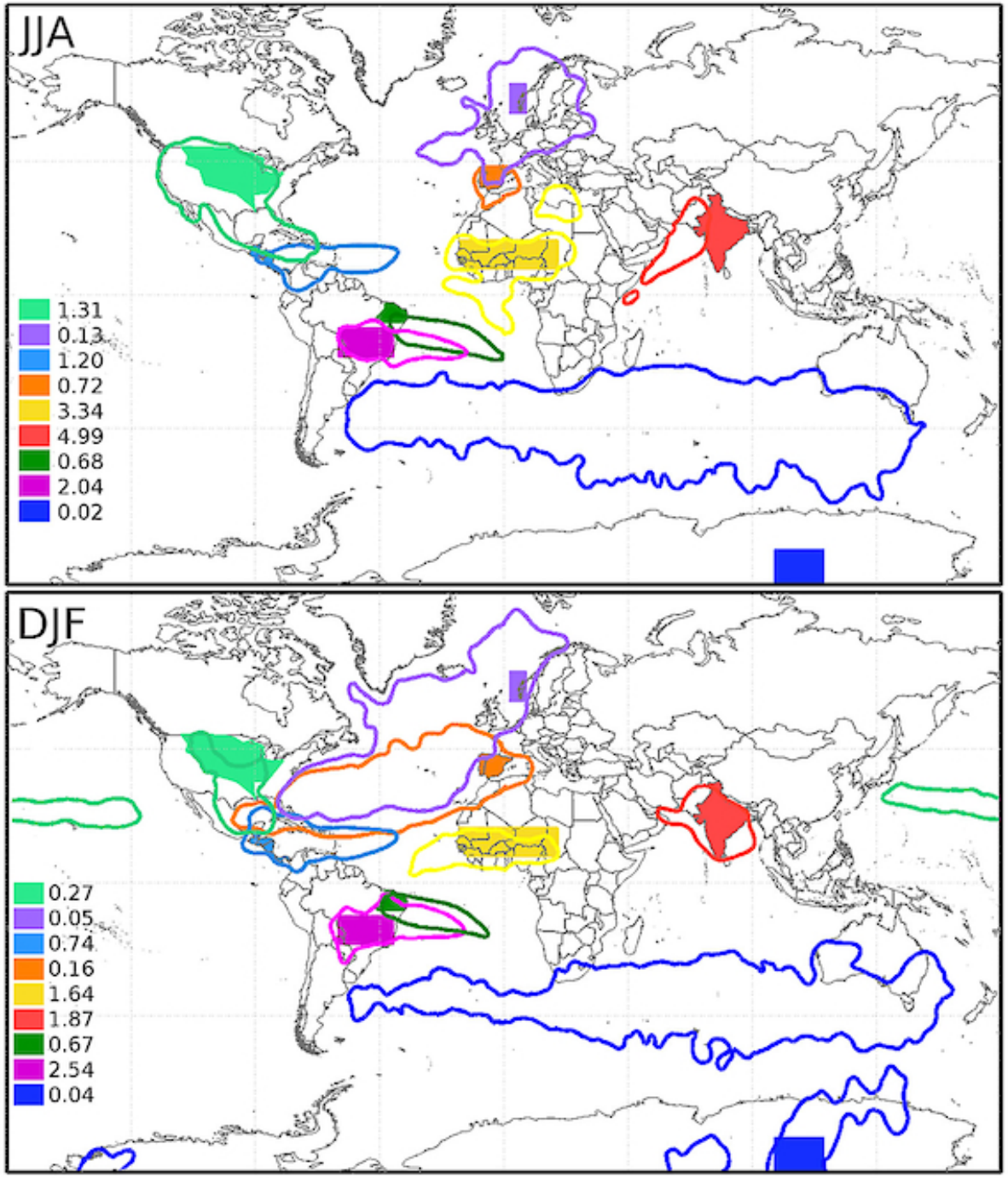


*Mean 10 day backward vertical integrated net freshwater flux (E-P)−10 in mm d−2 (contours) for selected target regions (continental areas in solid colors) for 2000–2004 based on global FLEXPART runs using ECMWF operational analysis (the same data as in the global study by Gimeno et al. [2010a, 2011]) for (top) JJA (June, July, August) and (bottom) DJF (December, January, February). Each contour surrounds the area covered by 95% of the moisture particles that reach the corresponding target region.*

**2 dynamic/meteorological structures play the most important role in global moisture transport**

Atmospheric Rivers (ARs)

Low-Level Jets (LLJs)

Deviations from the “normal” moisture transport can lead to **droughts** when the moisture supply is interrupted or to **flooding** when the supply of moisture for precipitation is too great. Often, drought or wet conditions triggered by abnormal moisture transport can be enhanced and prolonged by evaporation feedback from the local land surface

## Low-Level Jets (LLJs)

Corredores de viento donde su máx de velocidad se localiza dentro del **primer km** de altura.

- **Regiones tropicales y subtropicales.**

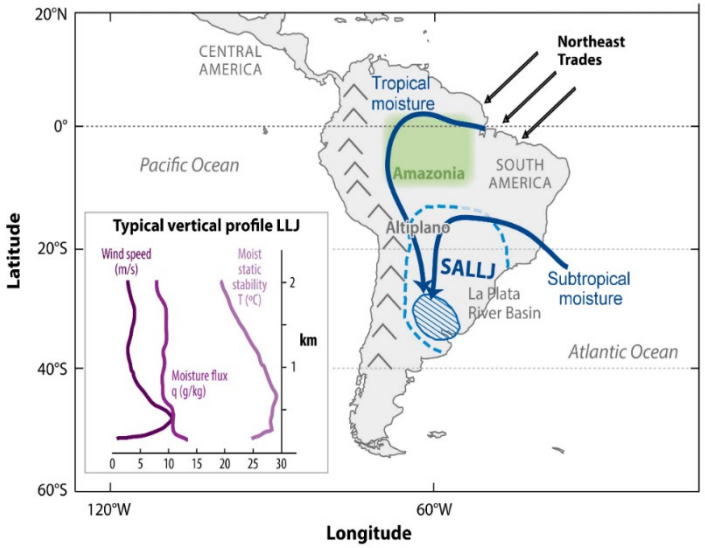


## Atmospheric Rivers (ARs)

Corredores alargados y estrechos de **transporte concentrado de humedad** asociados a ciclones extratropicales.

- El **90%** de la humedad que llega a latitudes extratropicales.

- **Regiones extratropicales.**

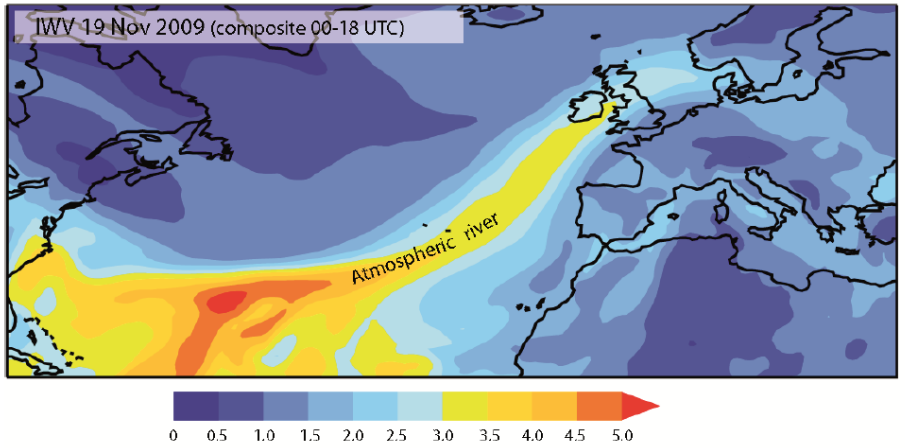


*Evap. Oceánica* → LLJ & ARs → Precipitaciones → *ANOMALIAS* → Extremos: sequías / inunciaciones

*transporte de humedad*

# Atmospheric Rivers

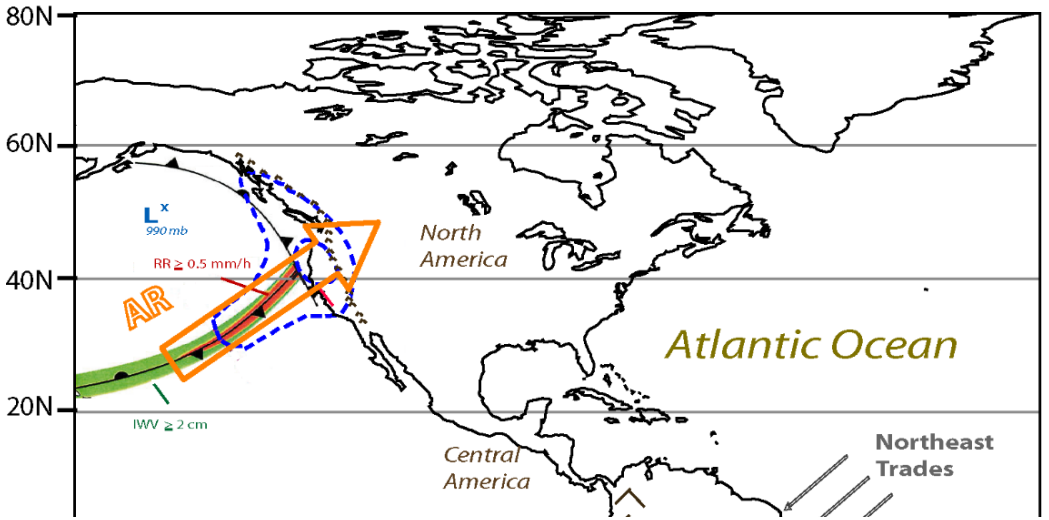


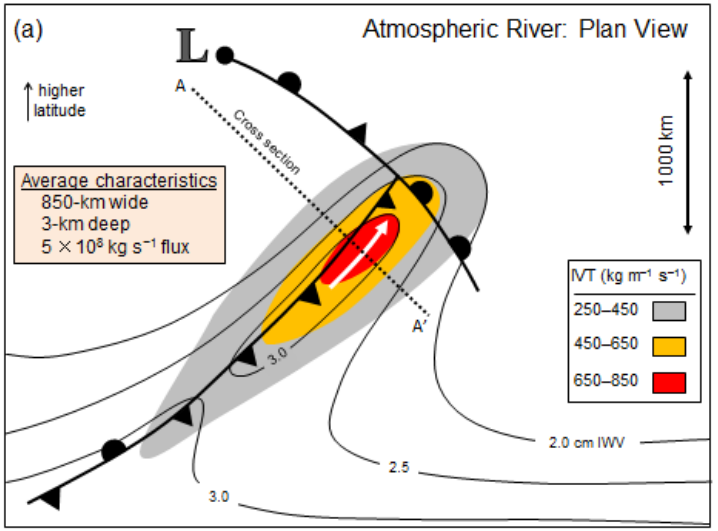


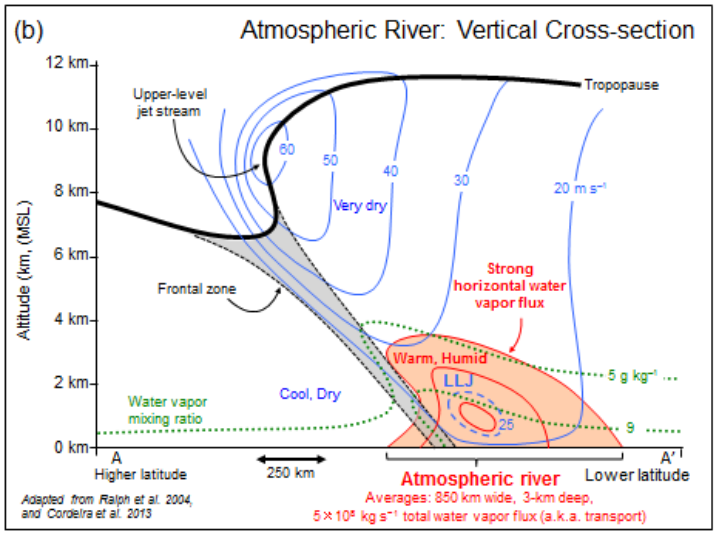


Corredor horizontal de alto contenido de vapor de agua
Fuertes vientos en niveles bajos
Largo: 2000 km
Ancho: 850km
Alto: 3 km

AMS, Glossary

Figure adapted from Gimeno et al. 2016, Major Mechanisms of Atmospheric Moisture Transport and their Role in Extreme Precipitation Events. Annual Review of Environmental and Resources.

**MOISTURE TRANSPORT** **EXTREME EVENTS**

MECHANISMS

Flooding and droughts

Often associated with extreme precipitation events are the **atmospheric rivers**.

The precipitation associated with such events is increased further when the AR impinges on a coastal mountain range, such as in California.

An example is shown in Figure where, as the flow is blocked by the mountain range, orographic lifting forces the moist air upward, and this can lead to extreme orographic precipitation. It also enhances the ascent associated with the warm conveyor belt.

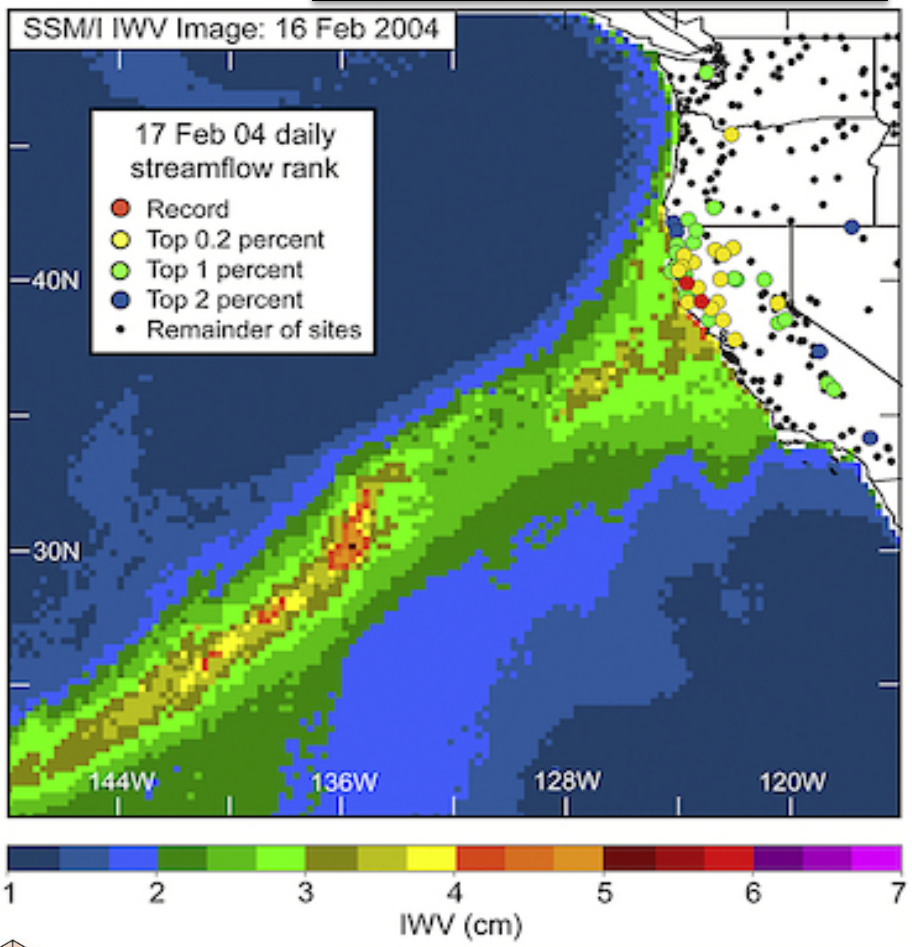


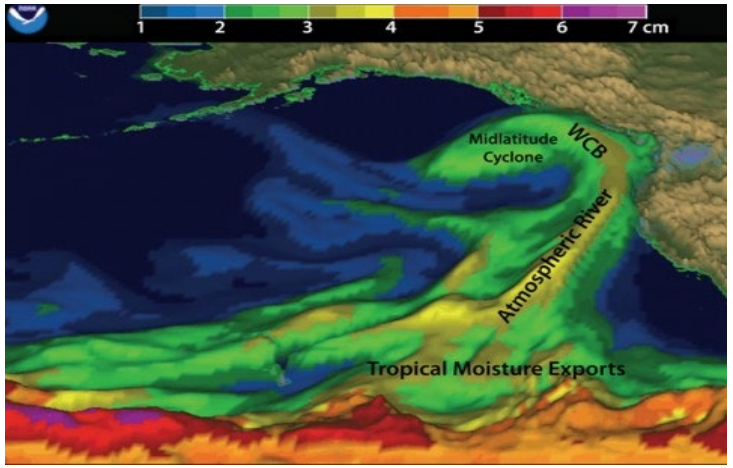


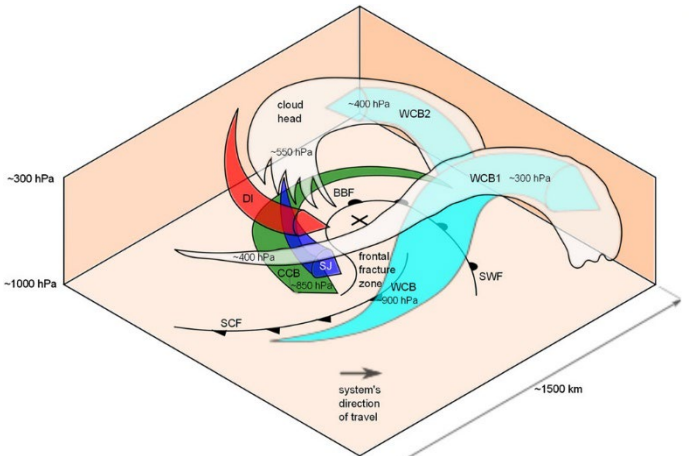


*Satellite observation of vertically integrated water vapor on 16 February 2004 and ranking of daily streamflows (percent; see inset key) on 17 February for those gauges that have recorded data for more than 30 years.*

# Atmospheric River

https://www.youtube.com/watch?v=NULrvr8pTBg

# The science behind atmospheric rivers

An atmospheric river (AR) is a flowing column of condensed water vapor in the atmosphere responsible for producing significant levels of rain and snow, especially in the Western United States. When ARs move inland and sweep over the mountains, the water vapor rises and cools to create heavy precipitation. Though many ARs are weak systems that simply provide beneficial rain or snow, some of the larger, more powerful ARs can create extreme rainfall and floods capable of disrupting travel, inducing mudslides and causing catastrophic damage to life and property. Visit www.research.noaa.gov to learn more.

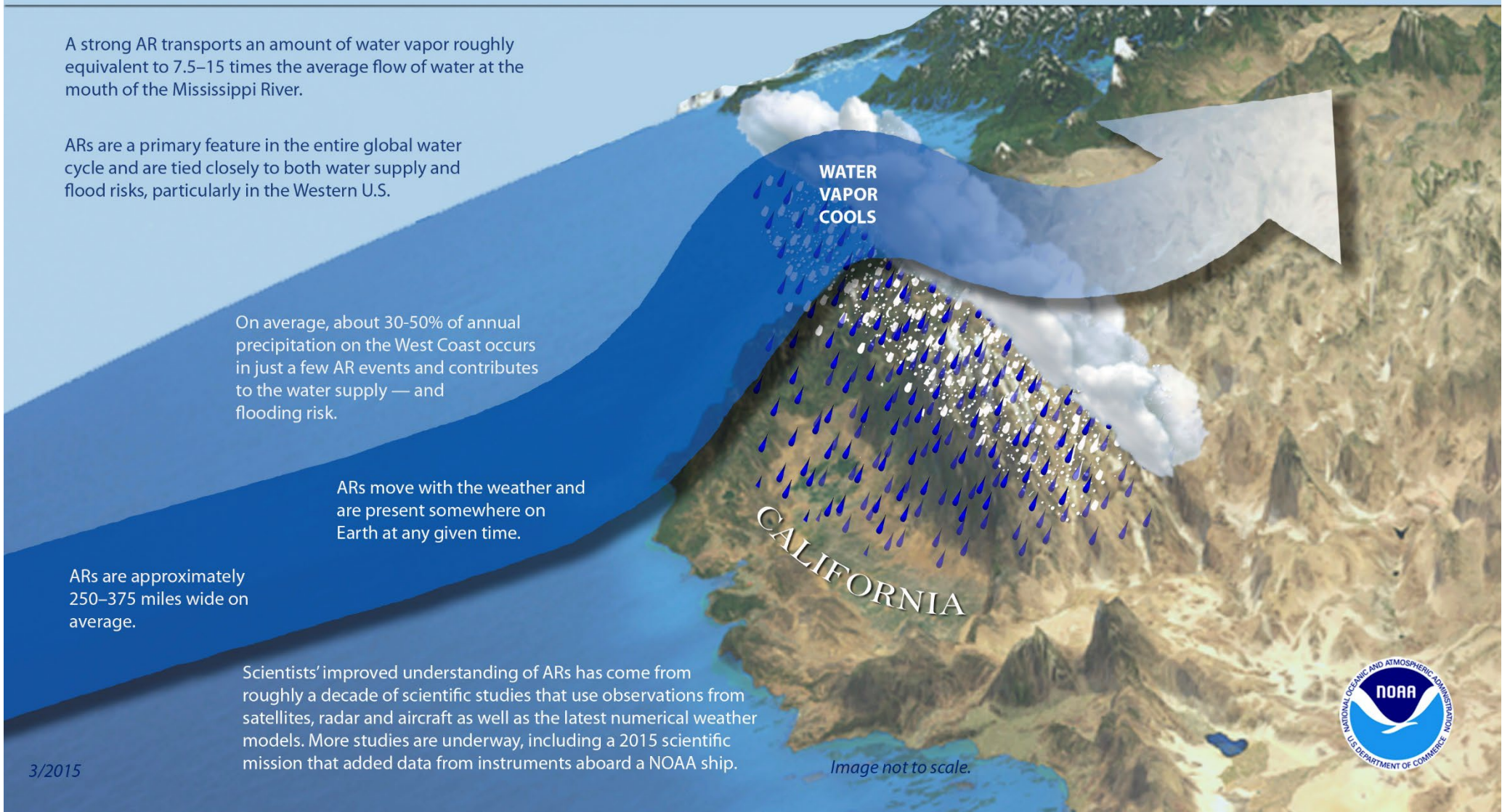

**MOISTURE TRANSPORT** **EXTREME EVENTS**

MECHANISMS

Flooding and droughts

https://cw3e.ucsd.edu/ivt_iwv_natlantic/

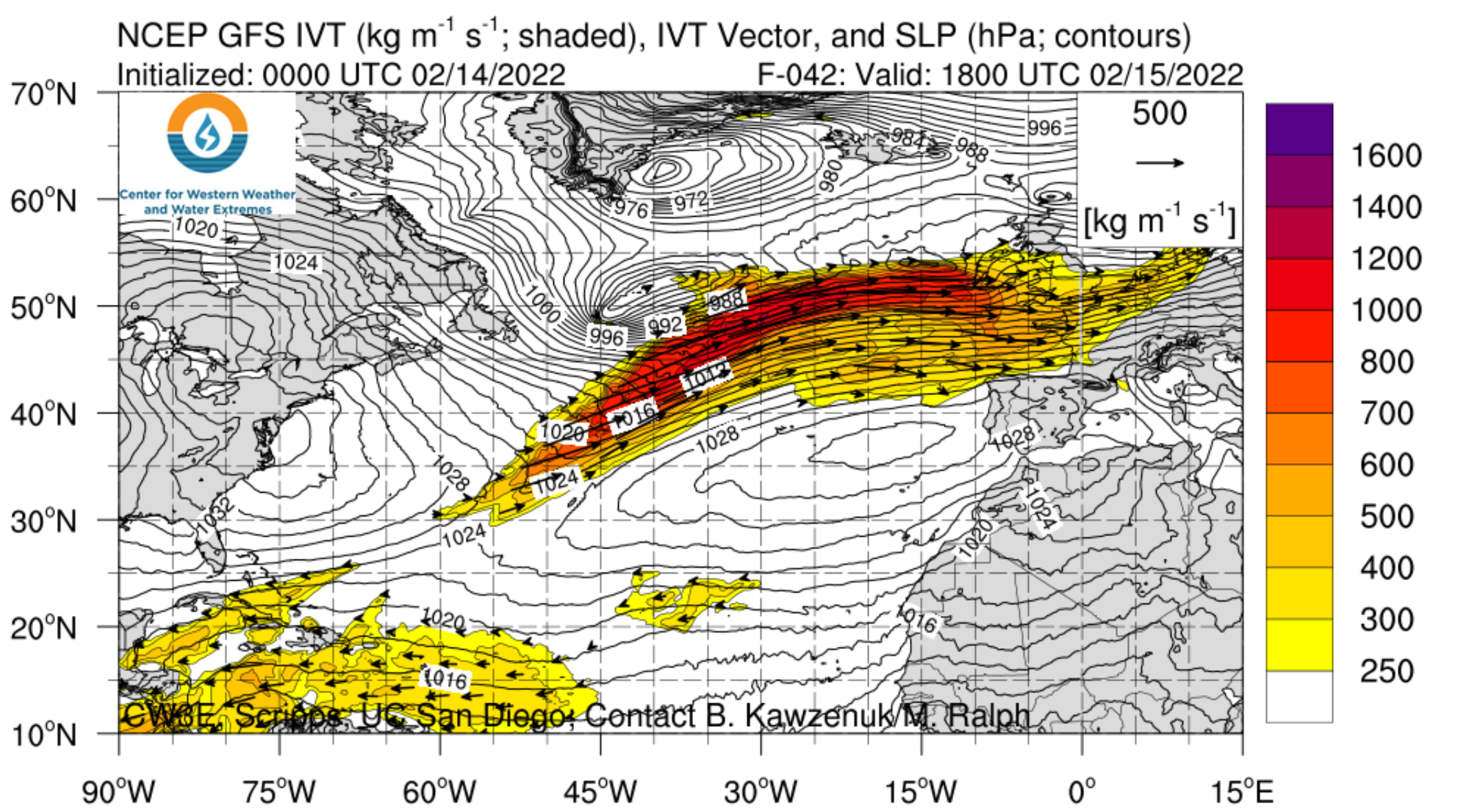

**MOISTURE TRANSPORT** **EXTREME EVENTS**

MECHANISMS

Flooding and droughts

## Water Year 2021 Precipitation Summary

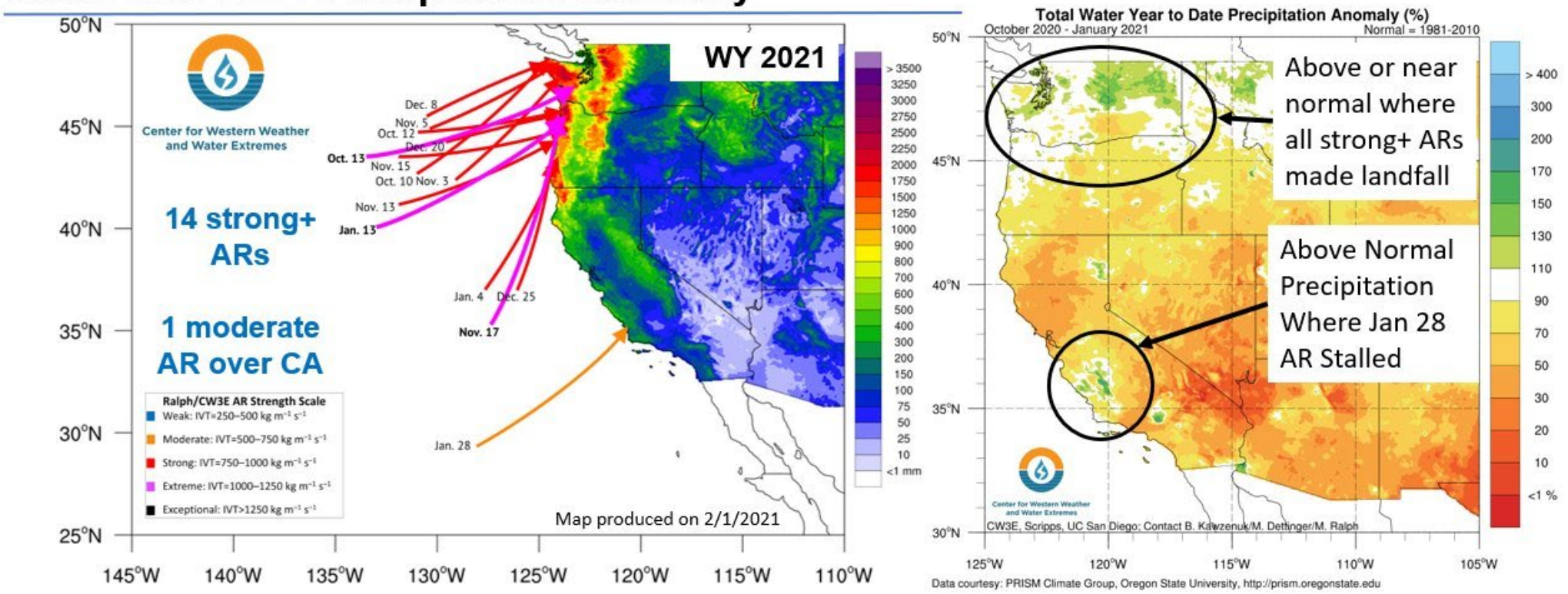





35 ARs have made landfall over the U.S. West Coast in the first 4 months of Water Year 2021.

While 35 is 6 more ARs than the same period last year, all but 2 were strongest over the Pacific Northwest, leaving CA dry.

The first southwesterly AR to make landfall over CA was strongest on January 28th.

This AR also stalled over the Central Coast, which is one of the few locations to receive above normal precipitation through January, highlighting how **only a few ARs can make or break a WY**.

*CW3E Scripps*

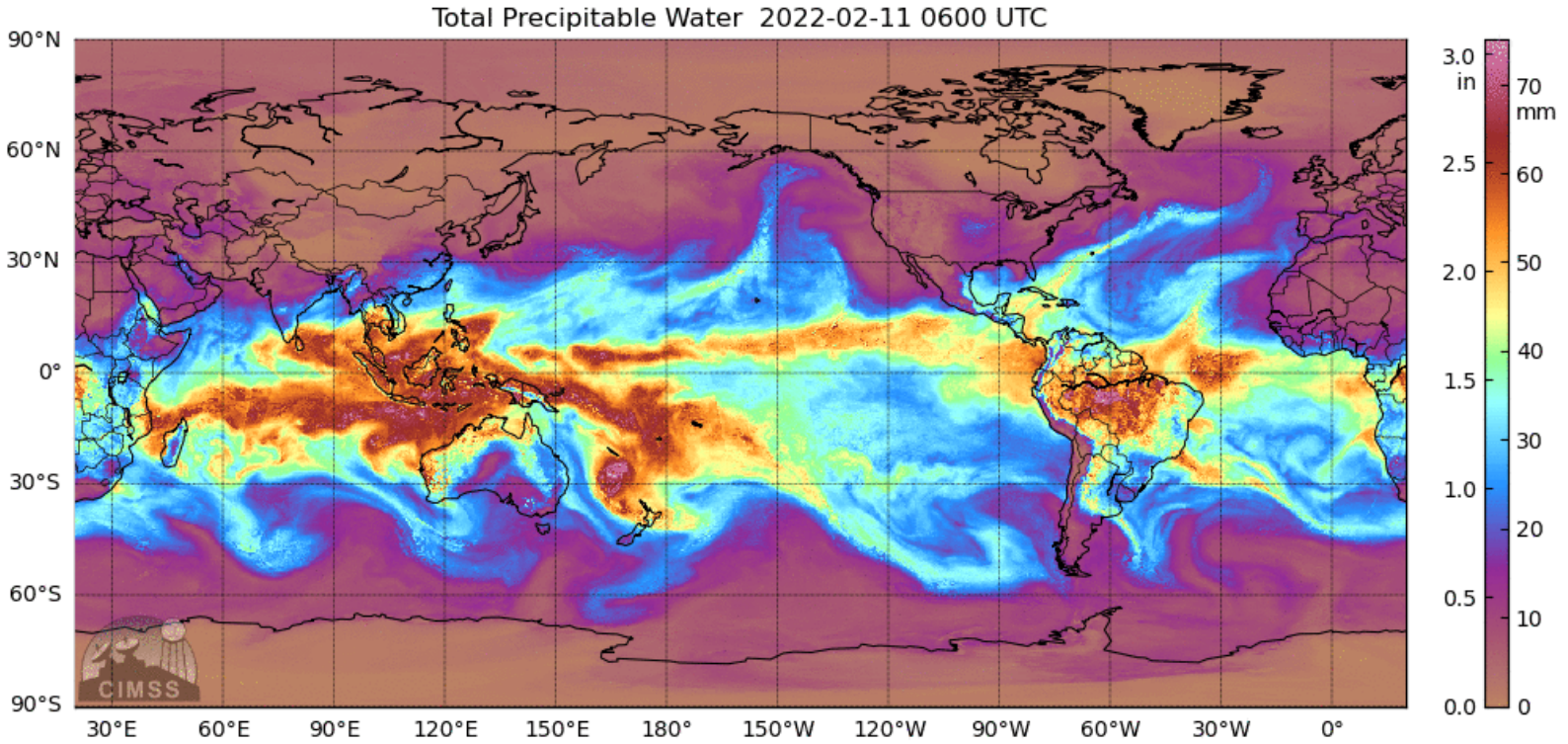


https://cw3e.ucsd.edu/images/ssmi/download/images/Global/GlobalAnim.gif

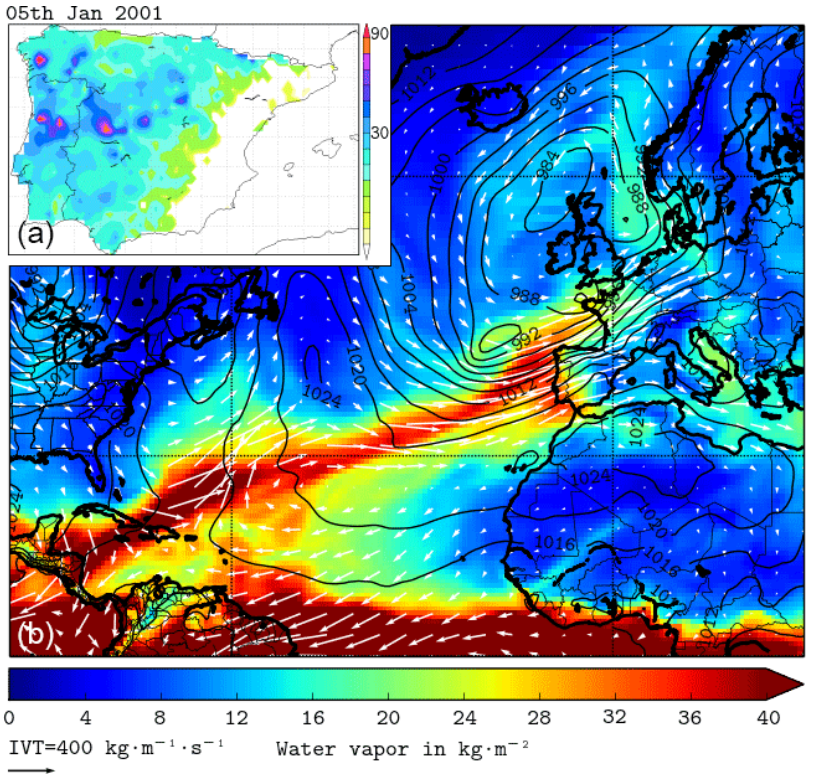


Existe una fuerte relación entre los ARs y la ocurrencia de los máximos anuales de días de precipitación en Europa (costa atlántica),

8 de cada top 10 máximos anuales de precip. está relacionado con un AR

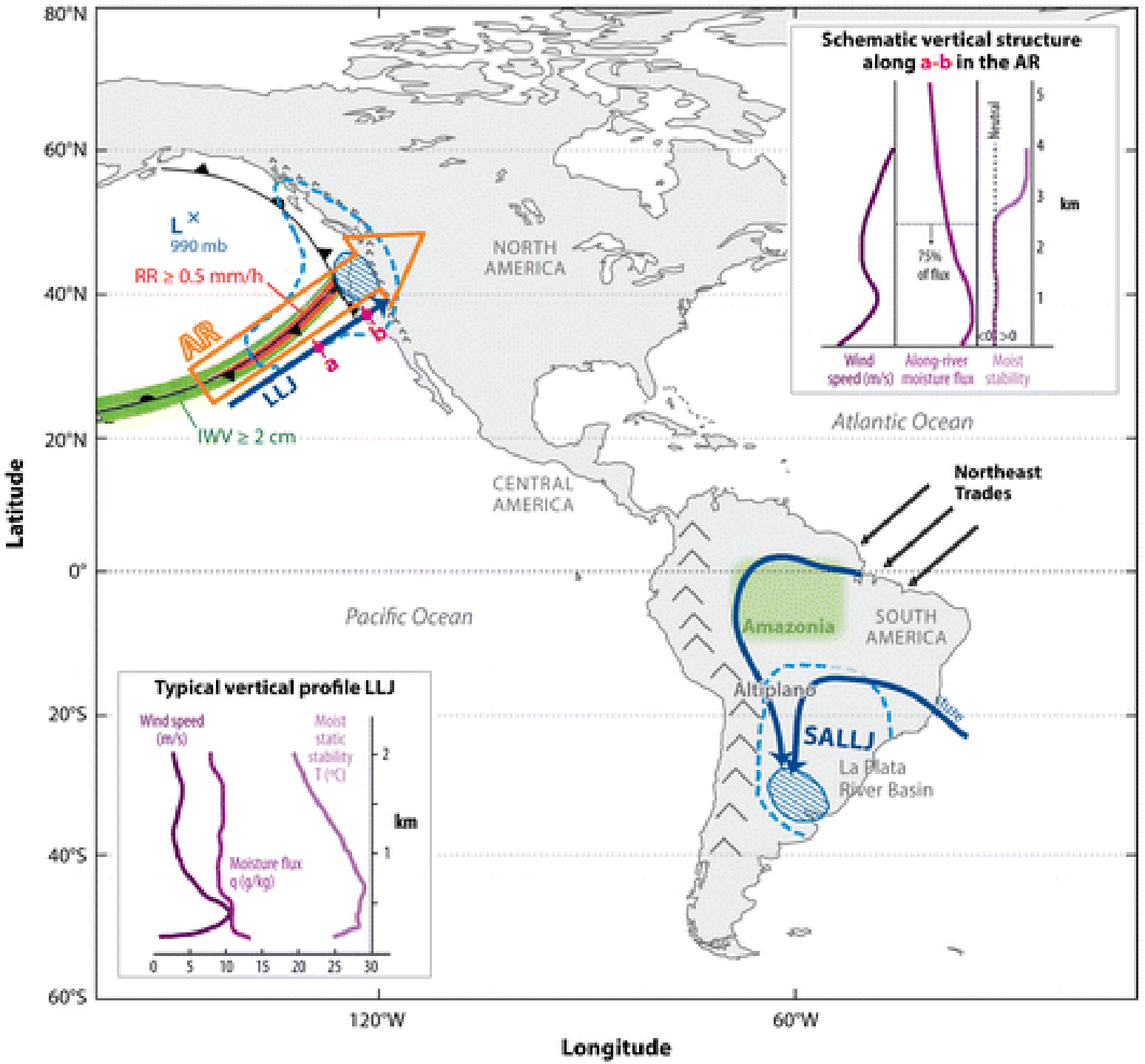


Gimeno L, et al. 2016.
Annu. Rev. Environ. Resour. 41:117–41

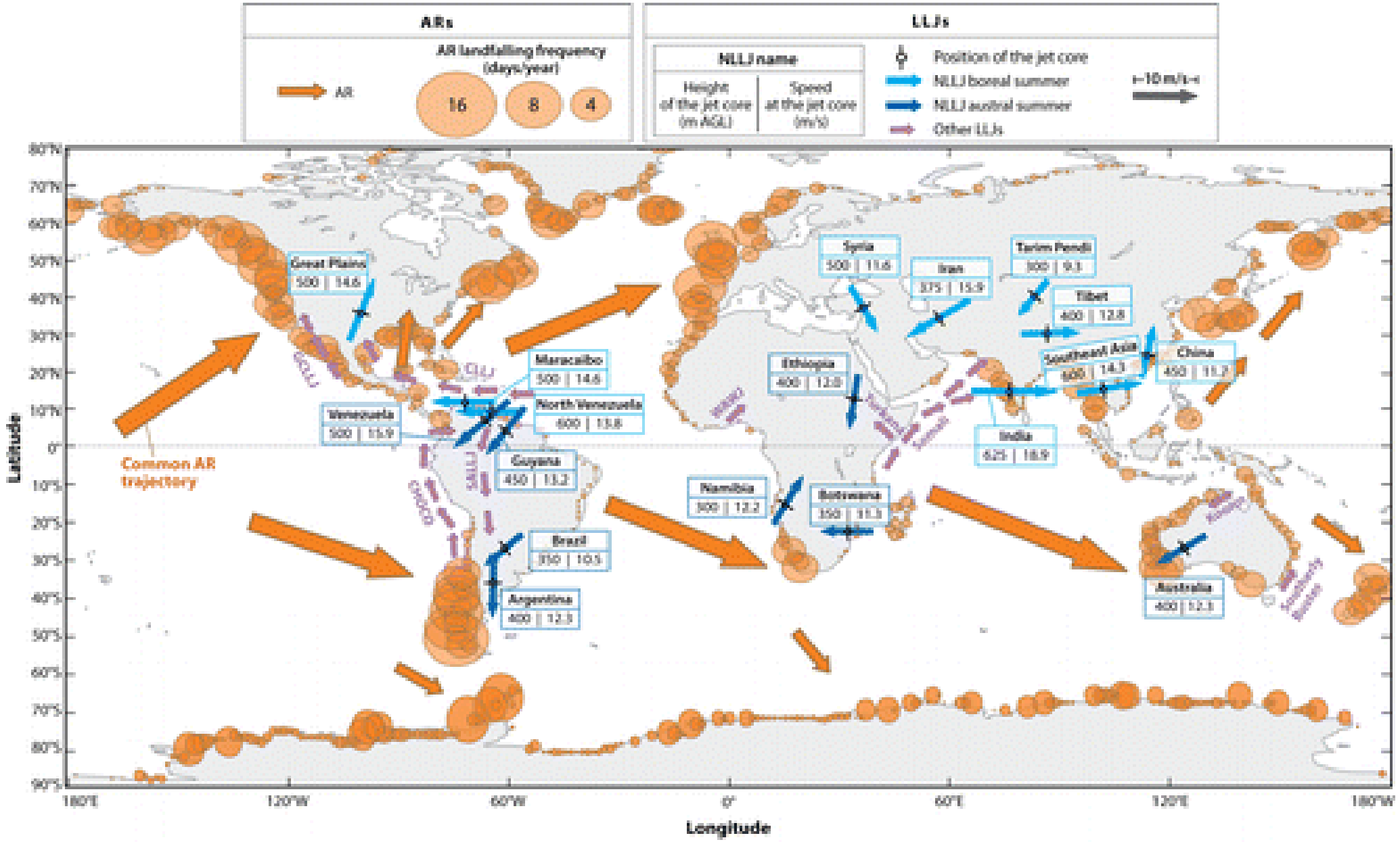


Gimeno L, et al. 2016.
Annu. Rev. Environ. Resour. 41:117–41

Caribean LLJ : CLLJ

**PERO**, ¿qué ocurre con las **ANOMALIAS DEL TRANSPORTE DE HUMEDAD**?

Existe un grado de incerteza con respecto a los mecanismos involucrados en las anomalías vistas durante eventos de precipitaciones extremas y sus consecuencias (ej. sequías e inundaciones).

**Sequias** → implican una cantidad menor significativa de humedad disponible con respecto a la media durante un periodo de tiempo prologado

**¿y su persistencia?** → puede ser debida en parte a una falta de humedad transportada hacia los continentes.

**Precipitaciones extremas e inundaciones** →

cantidades de humedad por encima de la media
+ convergencia

---

**¿CUAL ES EL PAPEL DE LOS MECANISMOS DE TRANSPORTE?**

# ¿Y SI SE PRODUCEN CAMBIOS?

# ¿Cambios Termodinámicos?

**ARs & LLJs** **modulan los patrones regionales y globales de precipitación** sobre los continentes, y tienen un papel clave en la **disponibilidad de los recursos hídricos**.

**El cambio de 1ºC provoca un cambio de aproximadamente un 7% en el contenido de vapor de agua.**

**Intensificación del Ciclo Hidrológico → mayor transporte de humedad**

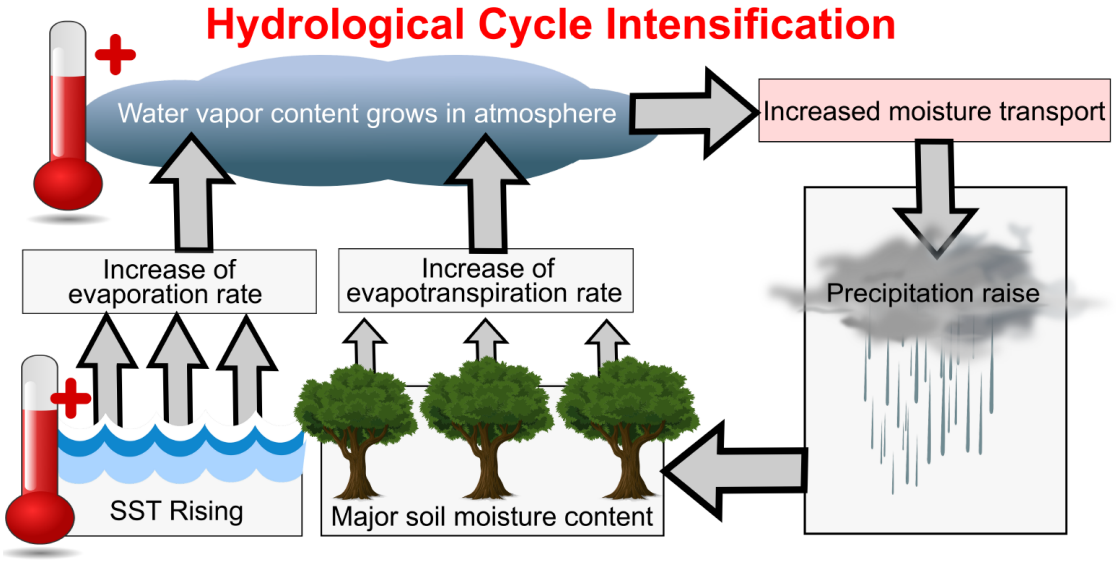


## ¿Cambios Dinámicos?

- **Lugares de ocurrencia**
- **Frecuencia**

**Anomalías** en el transporte de humedad → **Sequías extremas** o **precipitación intensa**

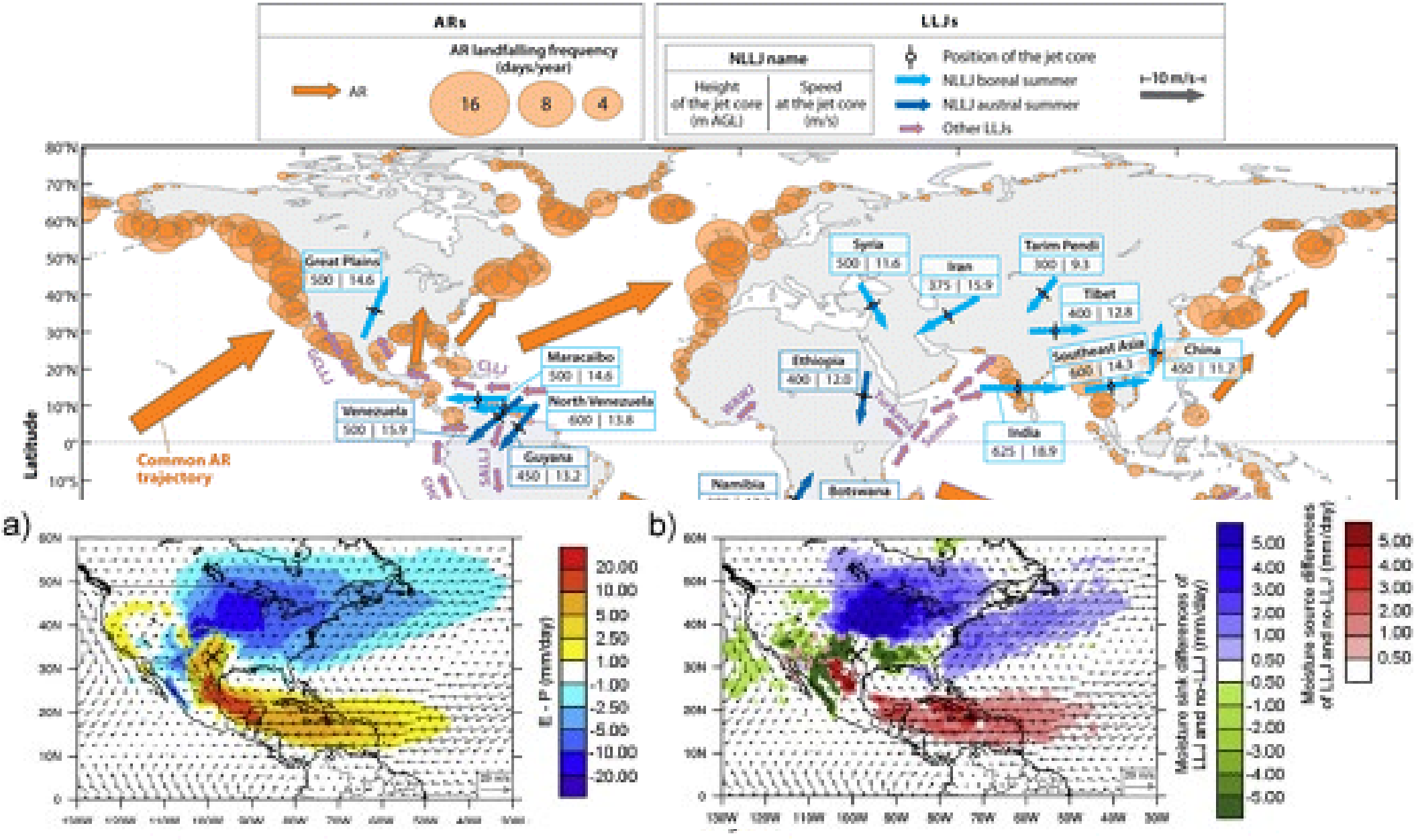


Gimeno L, et al. 2016.
Annu. Rev. Environ. Resour. 41:117–41

The **intensity of precipitation in monsoon regions** also depends strongly on the transport of water vapor from oceanic source regions.
Almost analogous to the situation in the midlatitudes, strong moisture transport, synoptically forced ascent, and topographically enhanced precipitation can lead to extreme events

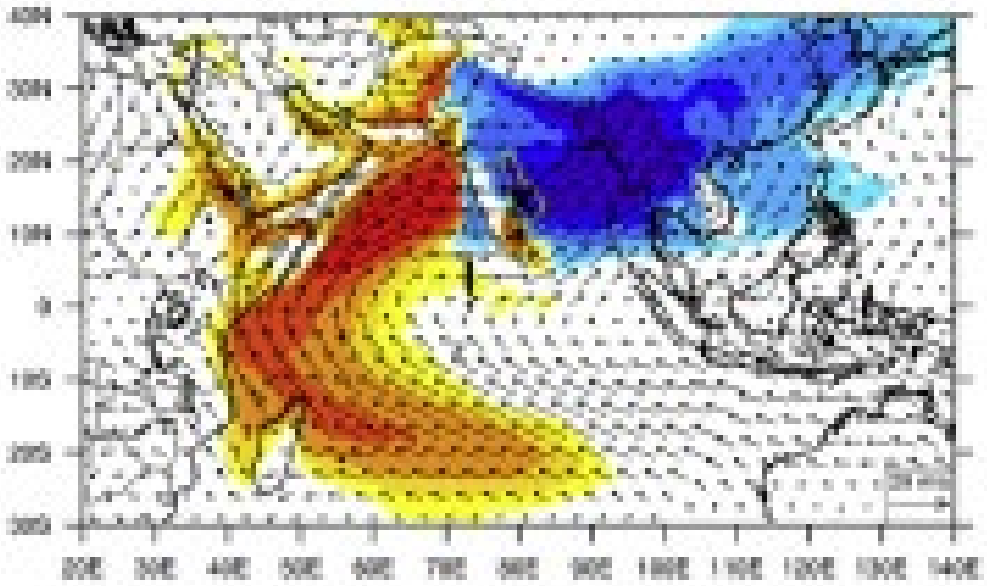

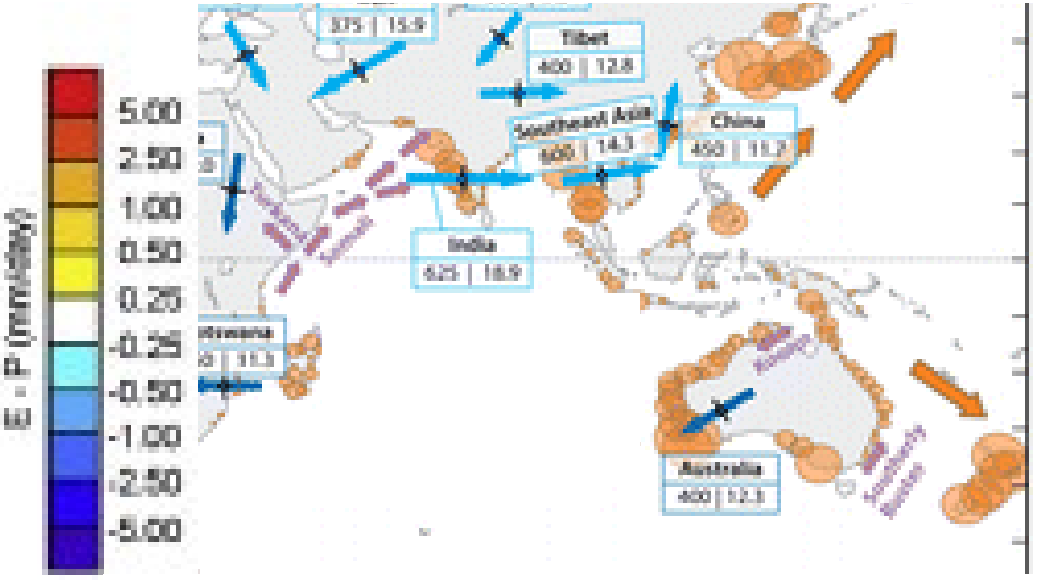


Gimeno L, et al. 2016.
Annu. Rev. Environ. Resour. 41:117–41

# EXTREME EVENTS



**Droughts,** on the other hand, are often caused by a diminished supply of water vapor from oceanic moisture source regions.

For example,

- ✓ a reduced intensity in northeast trade wind moisture transport into southern Amazonia was an important factor in the severe drought in Amazonia in 2005

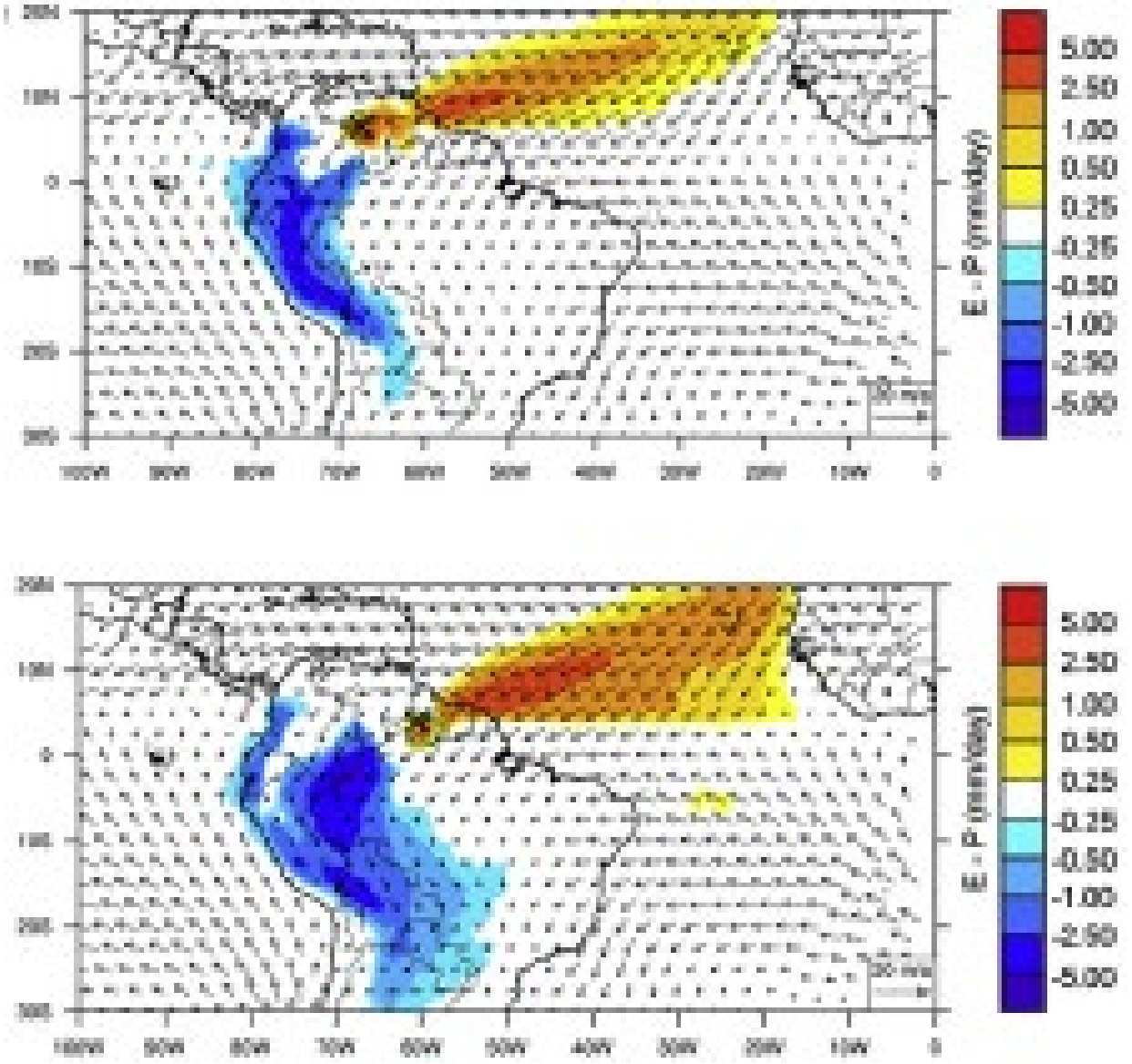

## Droughts,

- ✓ reduced tropical moisture transport is responsible for bad droughts in **southeast Australia**
- ✓ a reduction in moisture transport from the Arabian Sea was found to be linked with an **intense drought in India** in 2002
- ✓ For **northeast China**, it was shown that evaporation from the Yellow Sea is important for the variations in moisture inflow observed between years that are wetter or drier than normal

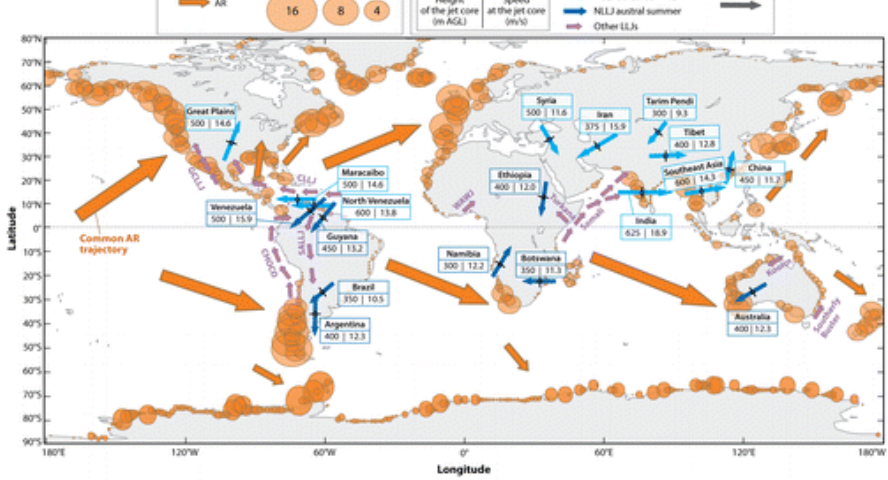


Gimeno L, et al. 2016.
Annu. Rev. Environ. Resour. 41:117–41

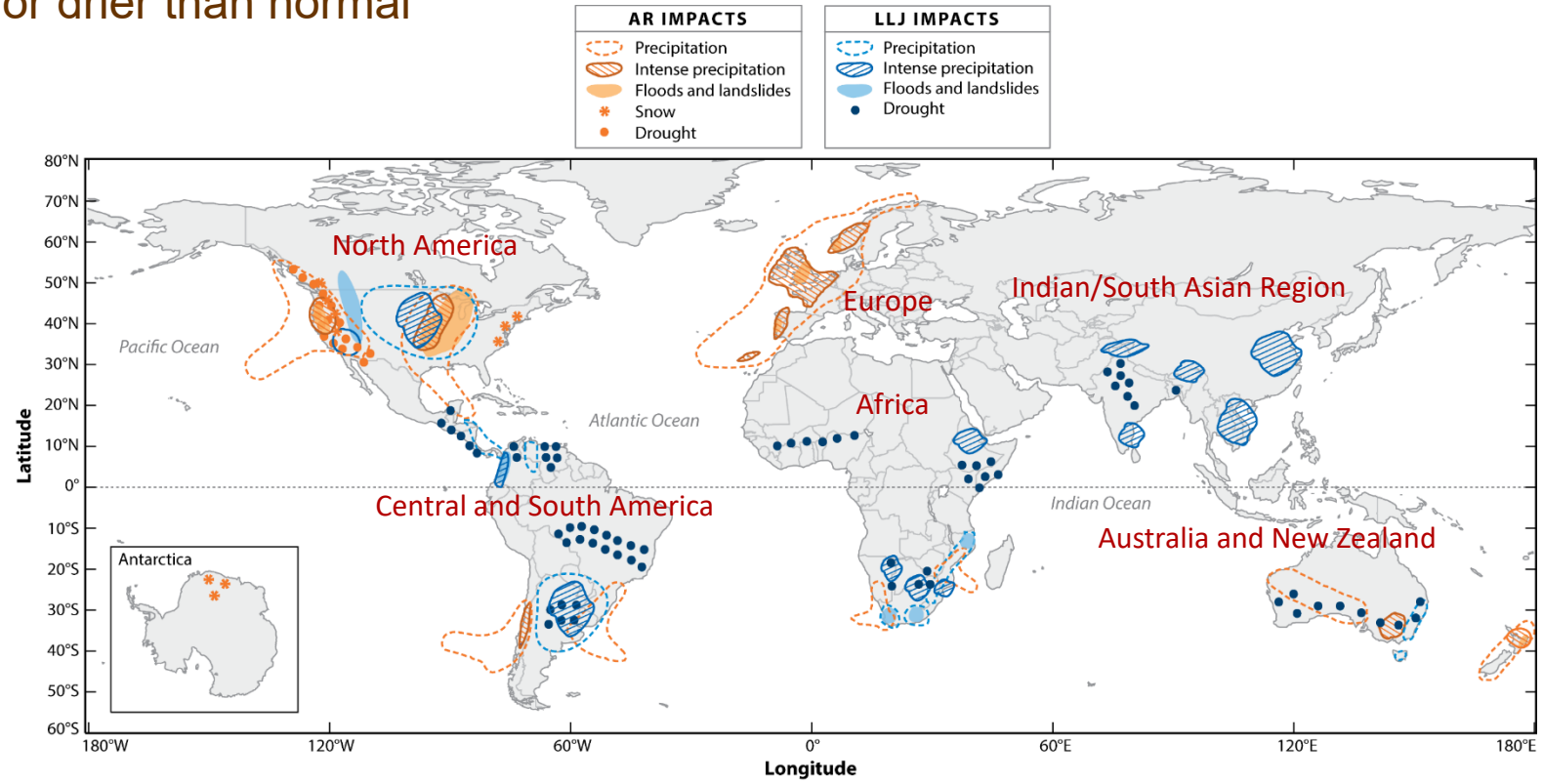


Gimeno L, et al. 2016.
Annu. Rev. Environ. Resour. 41:117–41

## CAMBIOS DINAMICOS Atmospheric Rivers

- **Lugares de ocurrencia**
- **Frecuencia**

} ARs

En general, los estudios apuntan a que los ARs serán **más fuertes y frecuentes**

No sólo aumentarán en intensidad y frecuencia los fenómenos extremos asociados (inundaciones, sequías), sino que también **puede estar en juego el equilibrio hidrológico a escala regional**.

Sin embargo, debido a su **dependencia de los procesos a escala meteorológica y climática**, las proyecciones son inciertas.

Payne, A.E., Demory, ME., Leung, L.R., Ramos, A.M., Shields, C.A., Rutz, J.J., Siler, N., Villarini, G., Hall, A., and Ralph, F.M. (2020). Responses and impacts of atmospheric rivers to climate change, Nat. Rev. Earth Environ., 1, 143–157, https://doi.org/10.1038/s43017-020-0030-5.

# IMPLICATIONS OF CLIMATE CHANGE -> global

- ✓ It has now become well established that **water vapor plays a major role in the climate of the planet**.

- ✓ In particular, **water vapor accounts for roughly 60% of the natural greenhouse effect** under clear skies.

- ✓ **Climate change scenarios** suggest that the high sensitivity of saturation vapor pressure to temperature **will result in an intensified hydrological cycle**, with **higher rates of evaporation and precipitation** in a warmer world.
  - ✓ This result follows directly from the C-C relationship.

- ✓ However, the response of the hydrological cycle is slightly **more complex**, and **thermodynamics alone cannot explain all of the predicted changes** in certain characteristics of the hydrological cycle.

- ✓ This means that **changes in atmospheric circulation** induced by global warming **will redirect moisture,** and **cause source-sink relationships of atmospheric water vapor** that **differ from the present case**.

- ✓ Those **continental regions that receive moisture from only one or two source region(s) may be more sharply exposed to changes** in water cycle due to changing climate than regions that draw on multiple moisture sources.

# Large Scale Circulation projected changes and their effect on the water cycle

## Poleward expansion of Hadley Cells

**Effect:** Broadening of the Hadley Cells and poleward expansion of subtropical dry zones

**Regions:** Uncertain influence on drying of subtropical land regions that are also controlled by evolving surface temperature patterns

**Confidence:** Low

## Poleward migration of storm tracks

Northern hemisphere


**Confidence:** Low

Southern hemisphere


**Confidence:** Medium

**Effect:** Annual-mean mid-latitude storm tracks shifting polewards.

**Regions:** Regional storm tracks moving polewards at different rates in different basins. Southern hemisphere storm tracks have moved polewards more clearly, partly driven by ozone depletion. Poleward movement likely to weaken as ozone hole recovers.

The maps show the effect of 3°C of global warming on mean P-E compared to preindustrial levels (1850-1900)

Annual mean

Seasonal mean

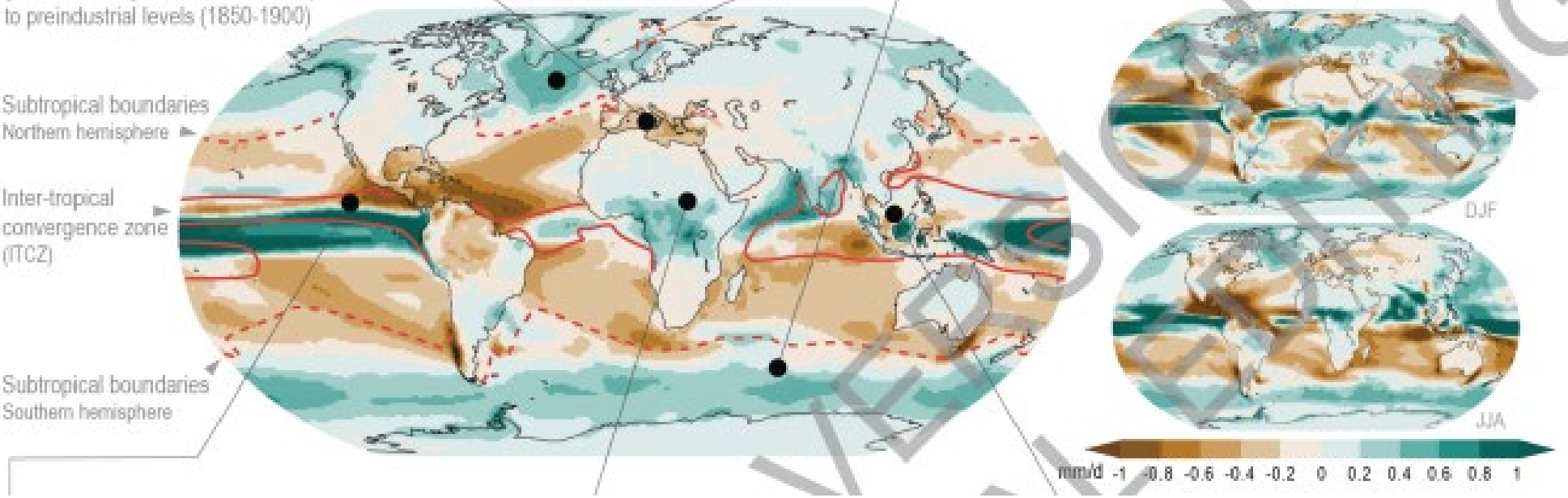




https://www.ipcc.ch/report/ar6/wg1/#FullReport

# ¿Y SI SE PRODUCEN CAMBIOS?

## Cambio proyectados e impactos de los ARs.

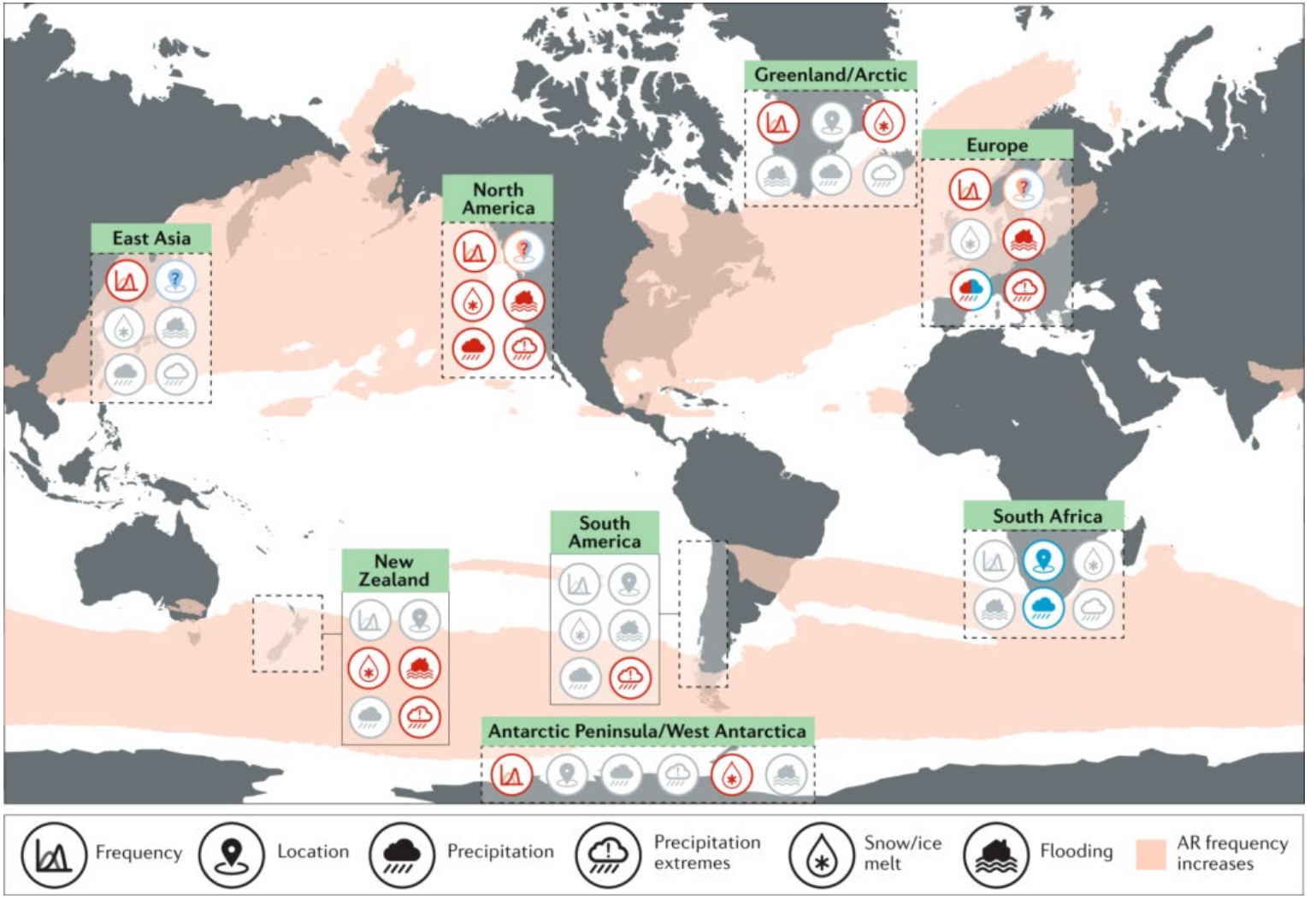


**Rojo -> incremento**

**Azul -> decrecimiento**

? -> incertidumbre en la proyección.

Gris -> cambios desconocidos

Payne et al. (2020). Responses and impacts of atmospheric rivers to climate change, Nat. Rev. Earth Environ.

# IMPLICATIONS OF CLIMATE CHANGE

Observed Changes

## Ocean evaporation

- ✓ Current best estimates of oceanic evaporation, such as those derived from the OAFlux data, show that a **strong increase in the overall rate of evaporation from the oceans has been occurring since 1978** (see Figure) and that this increase was **most pronounced during the 1990s**.

Oceanic evaporation (E ocean) trends from 1957 to 2015.

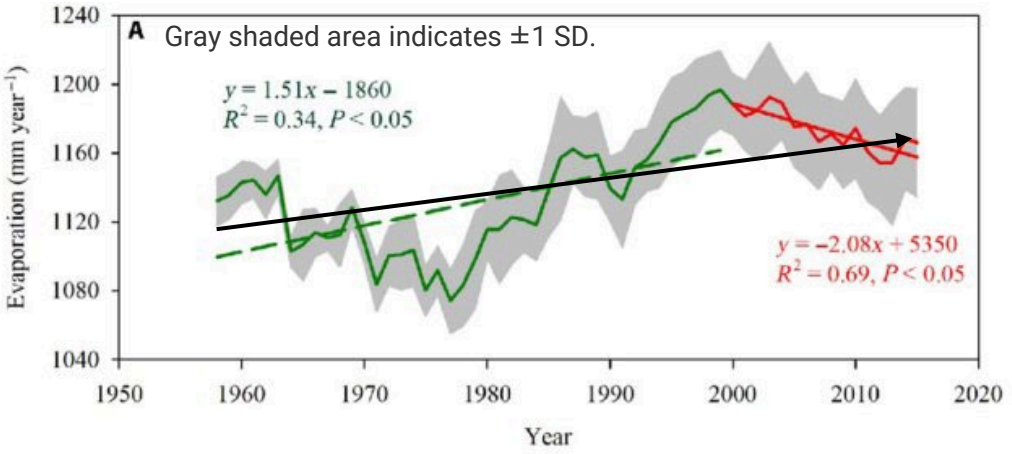


Spatial pattern on differences of oceanic evaporation trends between 1990s and 1970s.

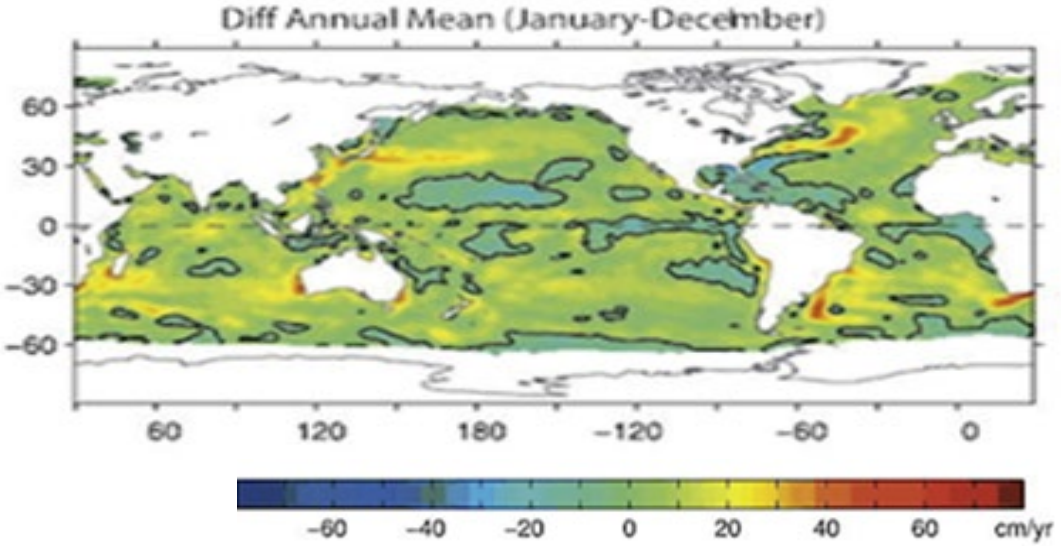


Yuan et al, 2019. Increased atmospheric vapor pressure deficit reduces global vegetation growth. Science Advances

# IMPLICATIONS OF CLIMATE CHANGE

Observed Changes

## Ocean evaporation

- ✓ While the **increase** in evaporation has occurred **at a global scale**,
- ✓ the spatial structures of the increase are **more coherent in winter** than in summer.

- ✓ The most significant of these are the:
  - ✓ **reduction** in evaporation **in the subtropics**,
  - ✓ the strong **increase** in evaporation along the paths of the global **western boundary currents**, and
  - ✓ the **increase** over the **Indo-Pacific warm pools**

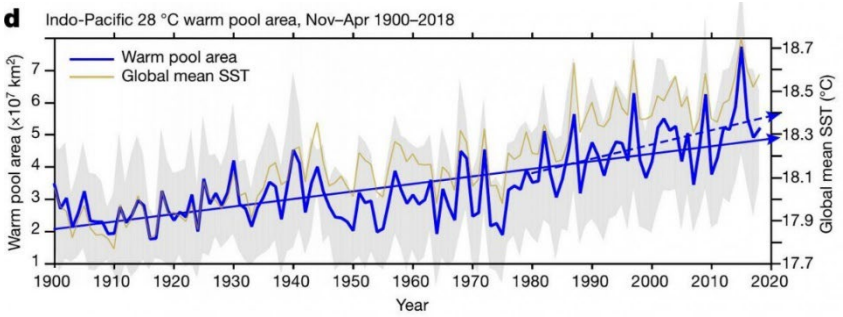


The extent of increase in Indo-Pacific warm pools is almost twofold.
The warm pool expanded from an area of $2.2 \times 10^7$ sq.km from 1900-1980 to $4 \times 10^7$ sq.km from 1981-2018.
The rate of expansion is $4 \times 10^5$ sq. km –> critical given the fact that these pools are the largest expanse of the warmest ocean temperatures on the planet

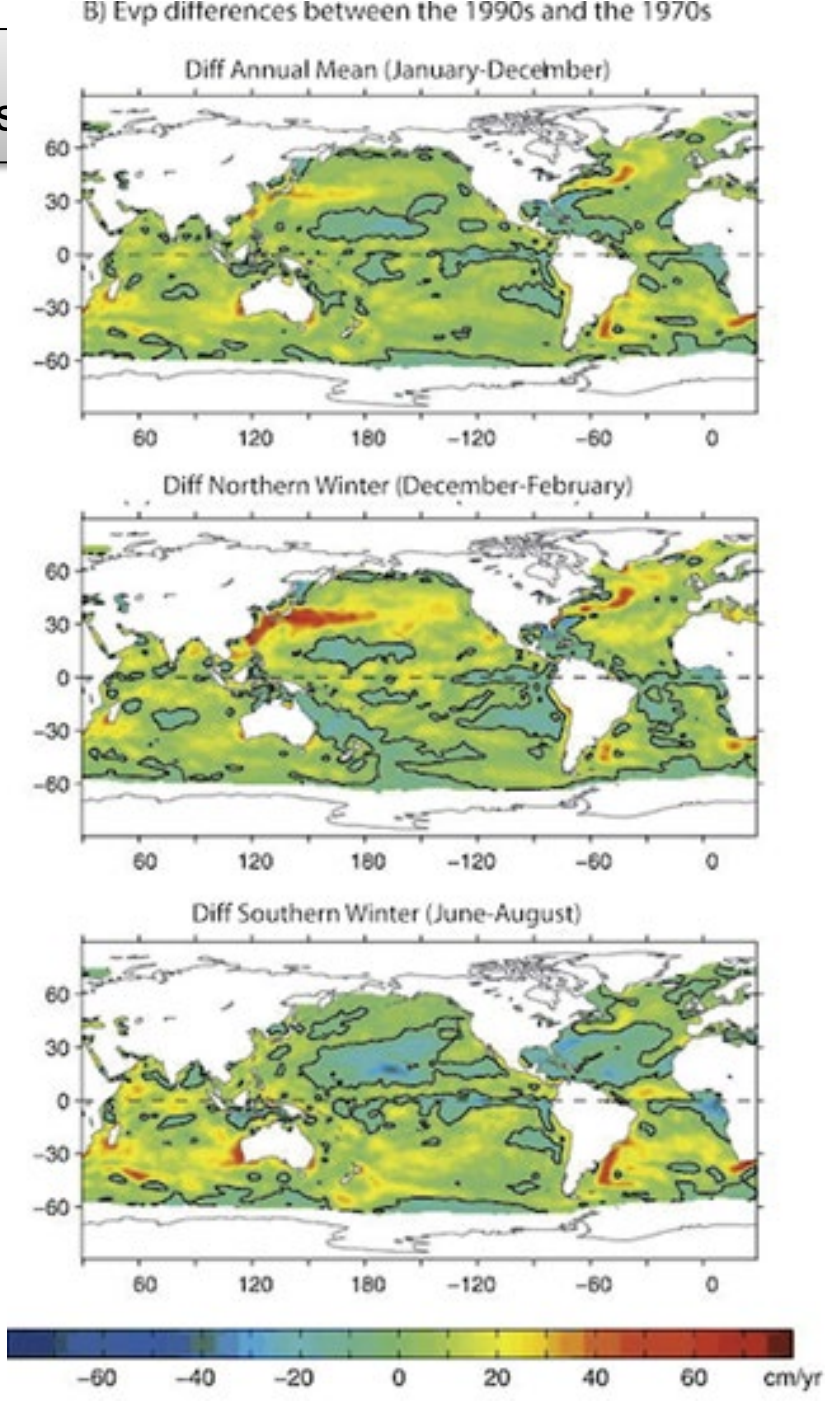


*Differences in evaporation between the 1990s and the 1970s. Zero contours are shown by thin black lines.*

# IMPLICATIONS OF CLIMATE CHANGE

Observed Changes

## Ocean evaporation

✓ **Decrease in the overall rate of evaporation from the oceans has been occurring since 1999**
(see Figure)

Comparison of oceanic evaporation (E ocean) trends during the two periods of 1957-1998 and 1999-2015.

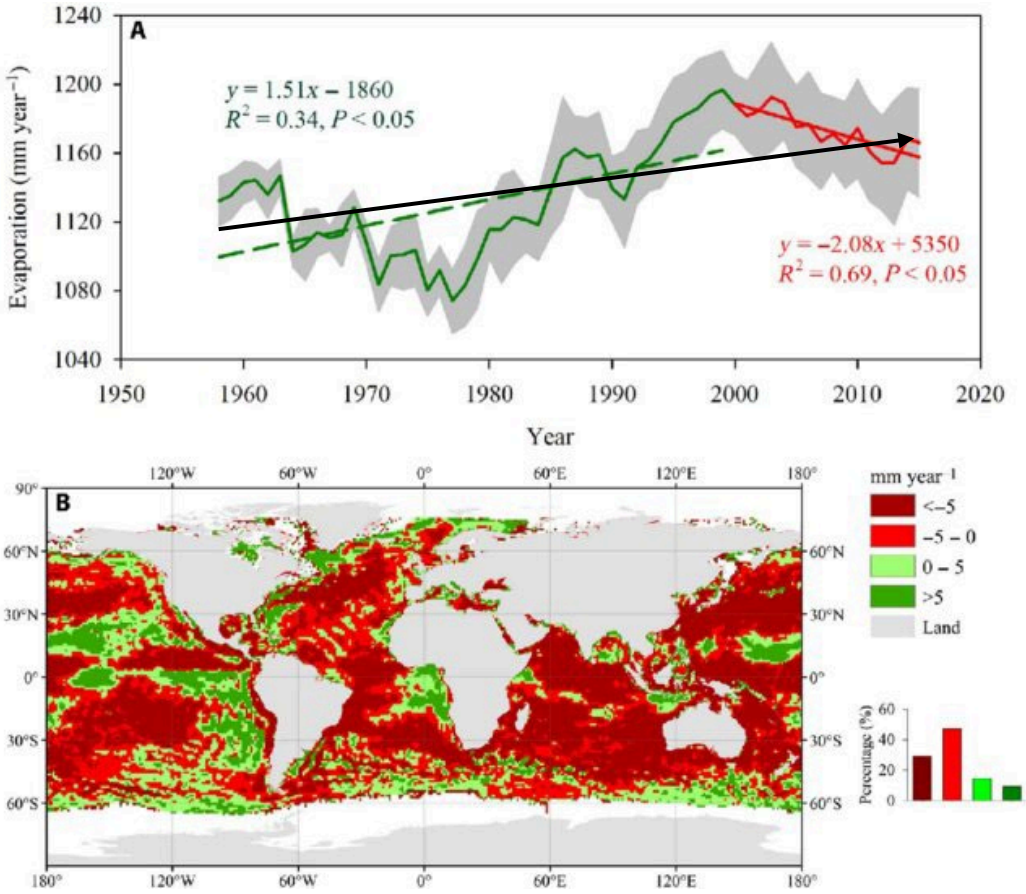


(A) Time series of globally averaged oceanic evaporation.
(B) Spatial pattern on differences of oceanic evaporation trends between 1999-2015 and 1957-1998.

Gray shaded area in (A) indicates ±1 SD.
The inset in (B) shows the frequency distributions of the corresponding differences.

•DOI: 10.1126/sciadv.aax1396

# IMPLICATIONS OF CLIMATE CHANGE

Observed Changes

## Water vapor

- ✓ The evolution of **vertically integrated water vapor** (precipitable water) has been derived from a number of different satellite data sets.
- ✓ The linear trend for the period 1988–2004 over the oceans was of the order of **1.2% per decade** (see Figure).
- ✓ However, the relatively short periods with available data, and strong interannual variability (often associated with El Niño events or large volcanic eruptions), affect the statistical significance of the trends.
- ✓ Nevertheless, the trends are **predominantly positive over the oceans**, and additionally suggest an El Niño–Southern Oscillation (ENSO) fingerprint.
- ✓ According to the latest Intergovernmental Panel on Climate Change (IPCC) report, **there was an overall growth of 5% in water vapor** throughout the entire 20th century, mostly due to increases during the last three decades.

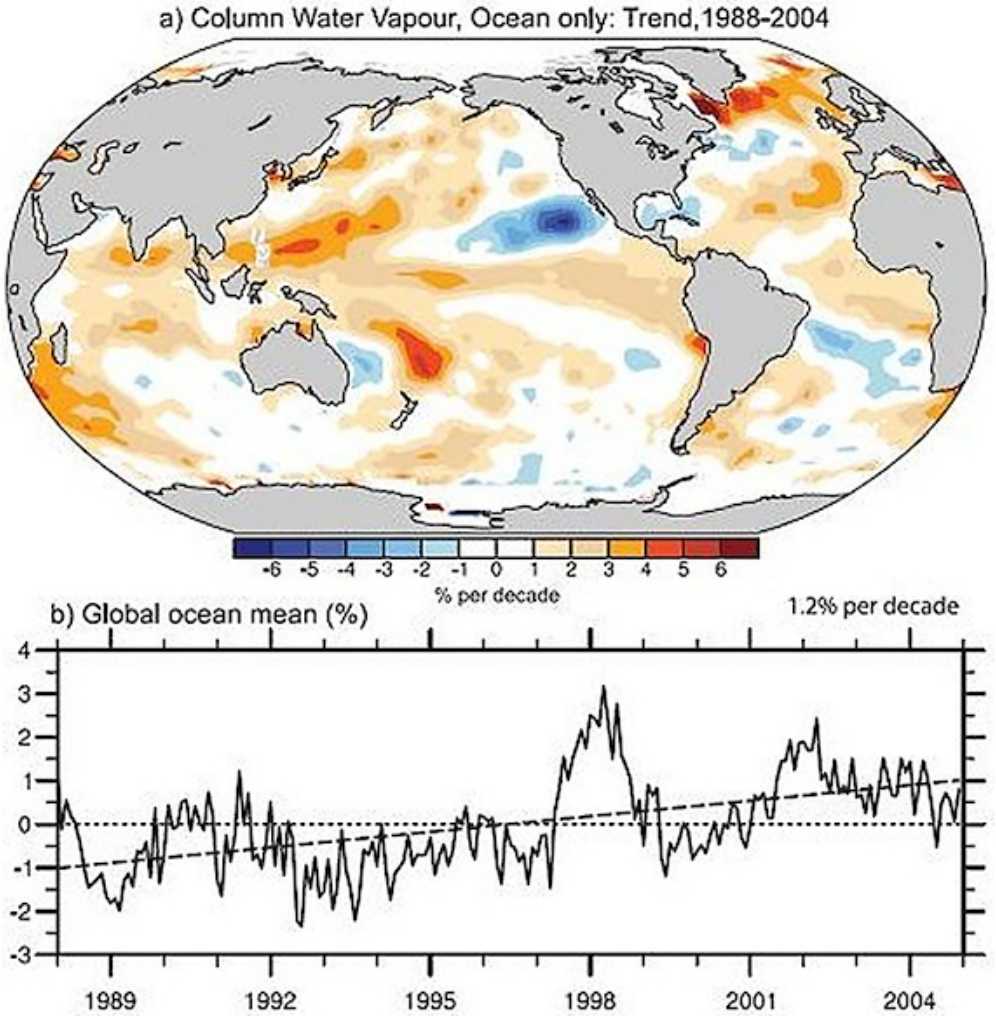


*(top) Linear trends in precipitable water (total column water vapor) in percent per decade and (bottom) monthly time series of anomalies relative to 1988–2004 in percent over the global ocean plus linear trend, from RSS SSM/I [from IPCC, 2007, chapter 3].*

# IMPLICATIONS OF CLIMATE CHANGE

Observed Changes

## Droughts

- ✓ There have been also changes in precipitation, aridity and soil moisture.
- ✓ According to recent analysis the global prevalence of **dry areas has increased significantly (1.74% per decade) since the 1950s**

GLOBAL PATTERN OF DROUGHT, AS MEASURED BY THE PALMER DROUGHT SEVERITY INDEX

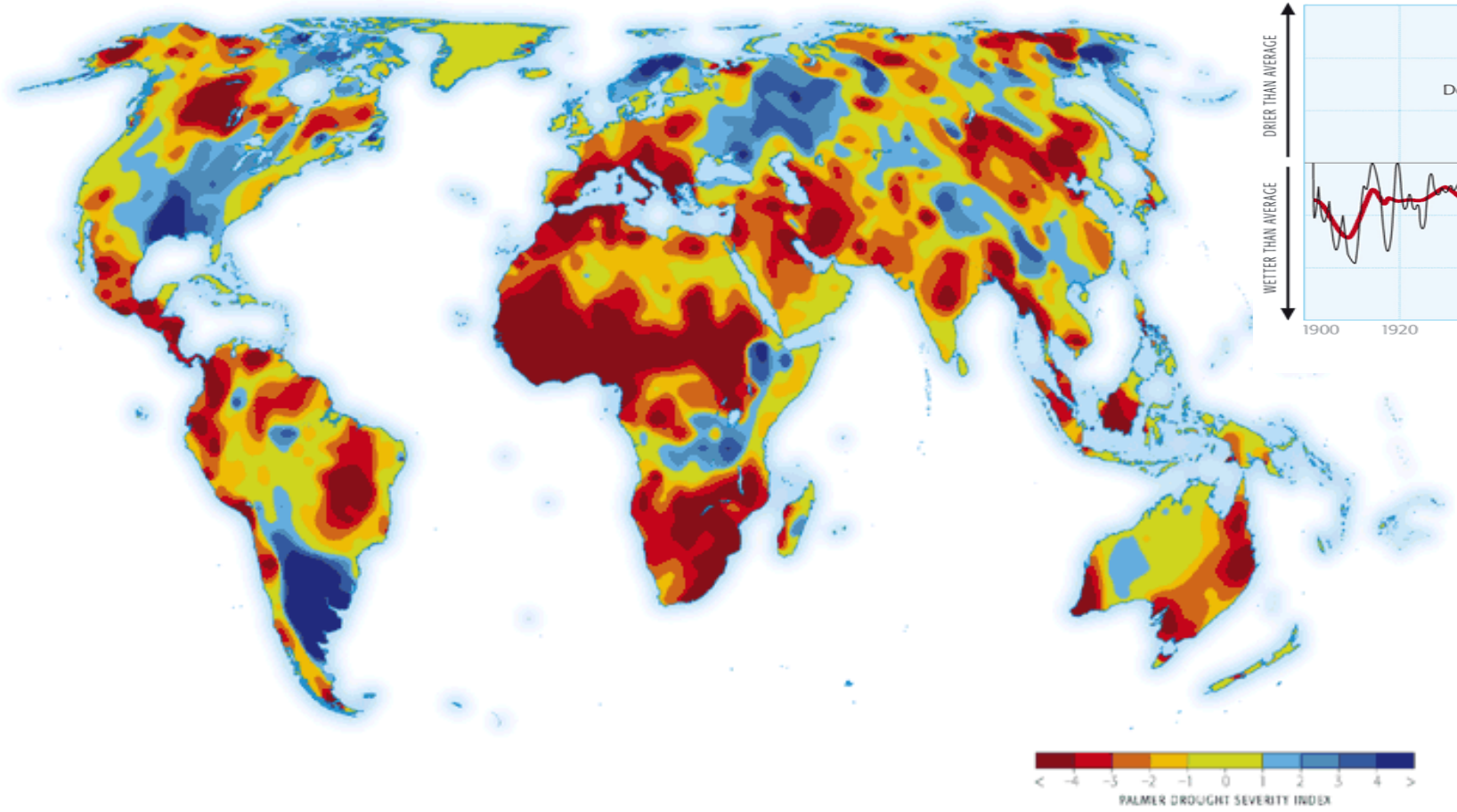


EVOLUTION OF DROUGHT PATTERN

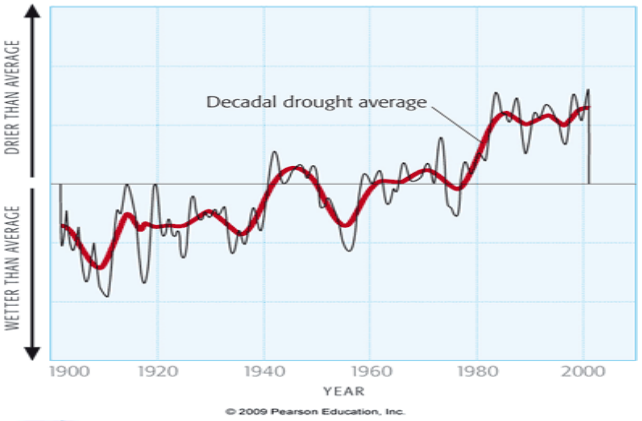


*Pearson, 2009*

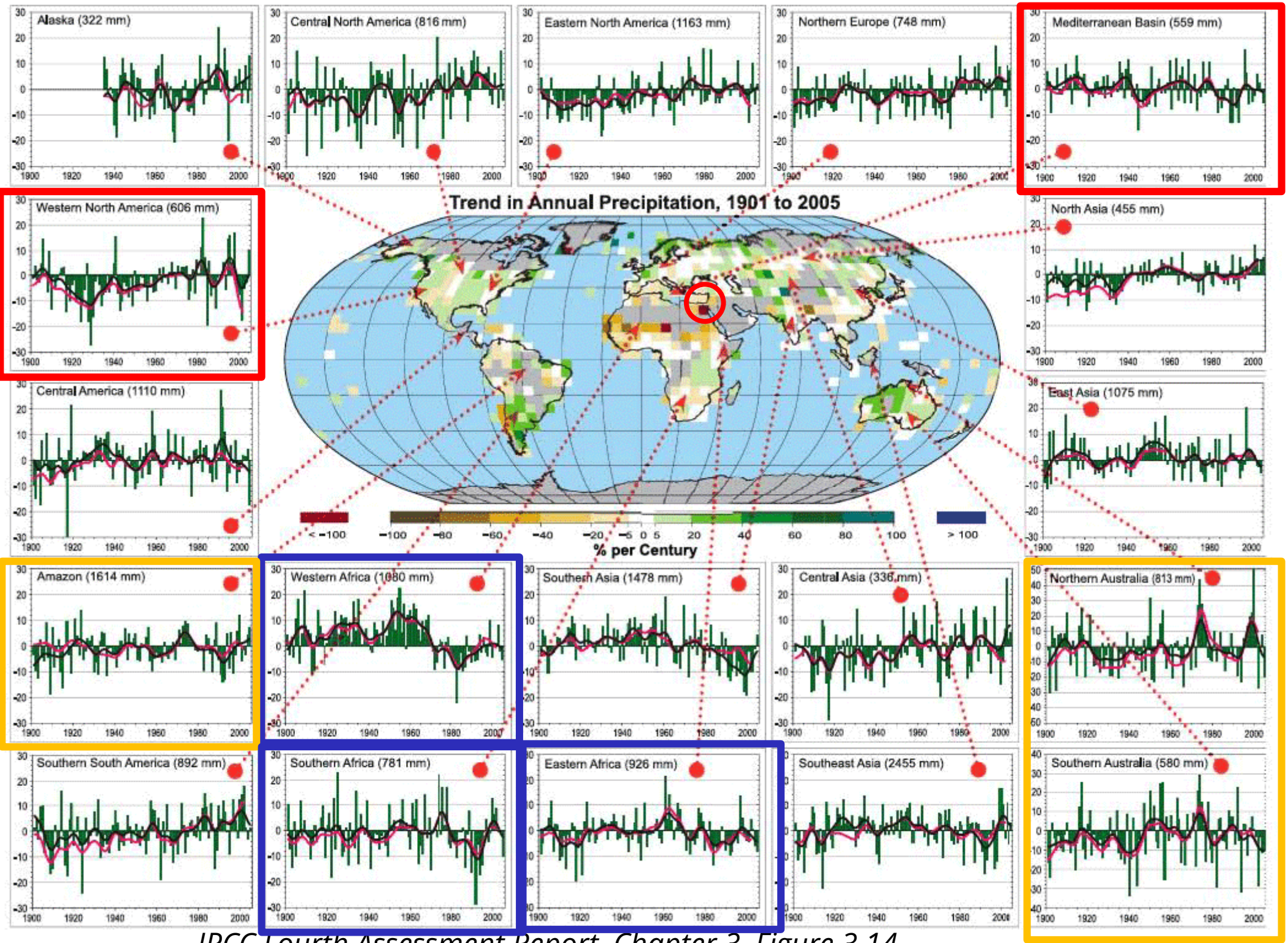


*IPCC Fourth Assessment Report, Chapter 3, Figure 3.14*

✓ Some of **this drying has occurred in highly populated areas of the world**, such as the **Mediterranean**, the **Fertile Crescent in the Middle East**, and **SW United States**. However, sparsely populated regions such as the **Amazon** and **Australia** have also been affected by an increasing frequency of extreme drought events.

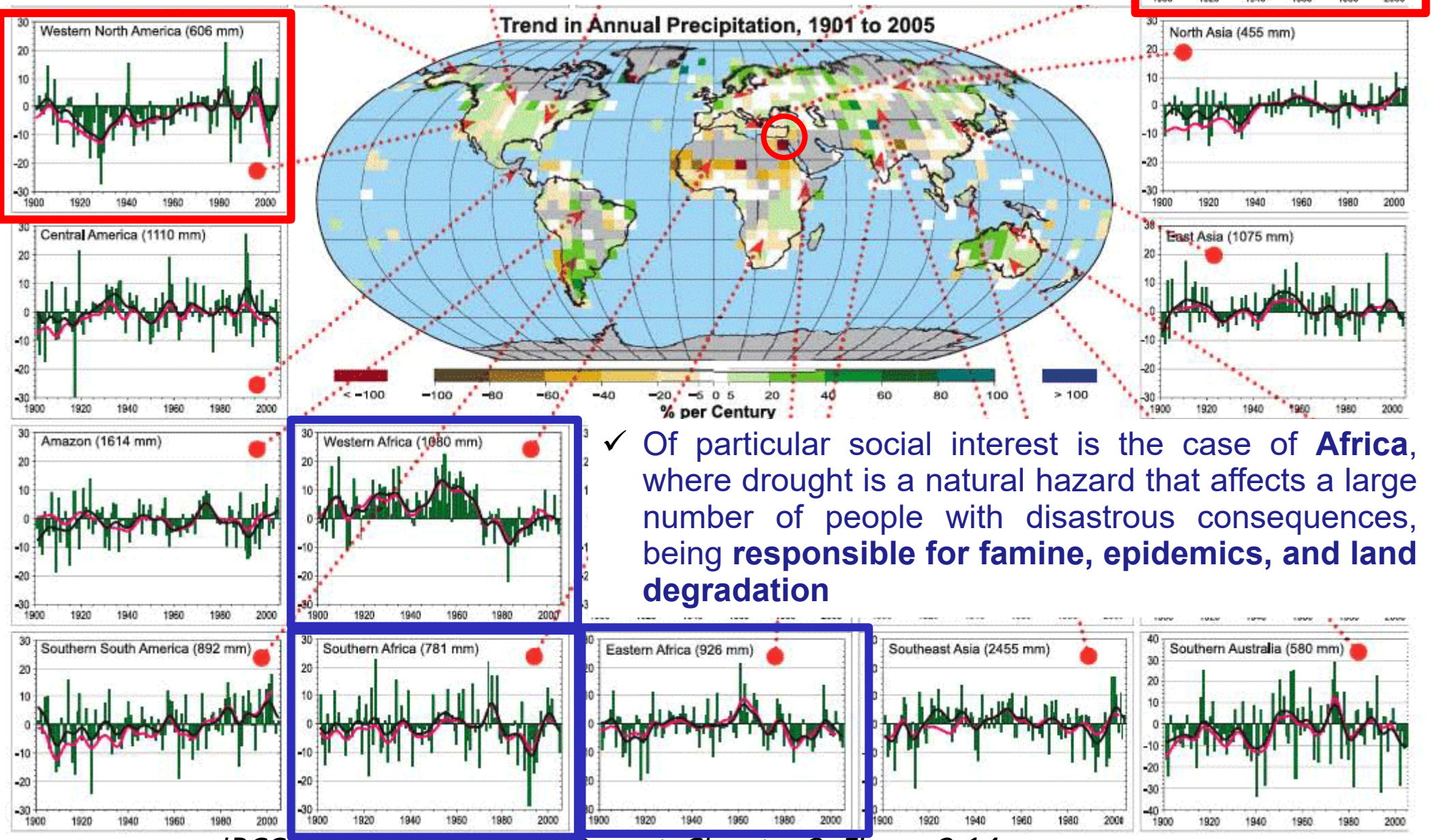


✓ Of particular social interest is the case of **Africa**, where drought is a natural hazard that affects a large number of people with disastrous consequences, being **responsible for famine, epidemics, and land degradation**

*IPCC Fourth Assessment Report, Chapter 3, Figure 3.14*

# IMPLICATIONS OF CLIMATE CHANGE

Observed Changes

## Droughts

- ✓ Among the most significant natural disasters affecting the world for the period 1974–2007, the two that resulted in the greatest number of deaths were the droughts that killed 450,000 and 325,000 people in Ethiopia/Sudan and the Sahel region in 1984 and 1974, respectively

- ✓ Interestingly, these very same areas are expected to become even drier in the coming decades according to the latest results published in IPCC reports

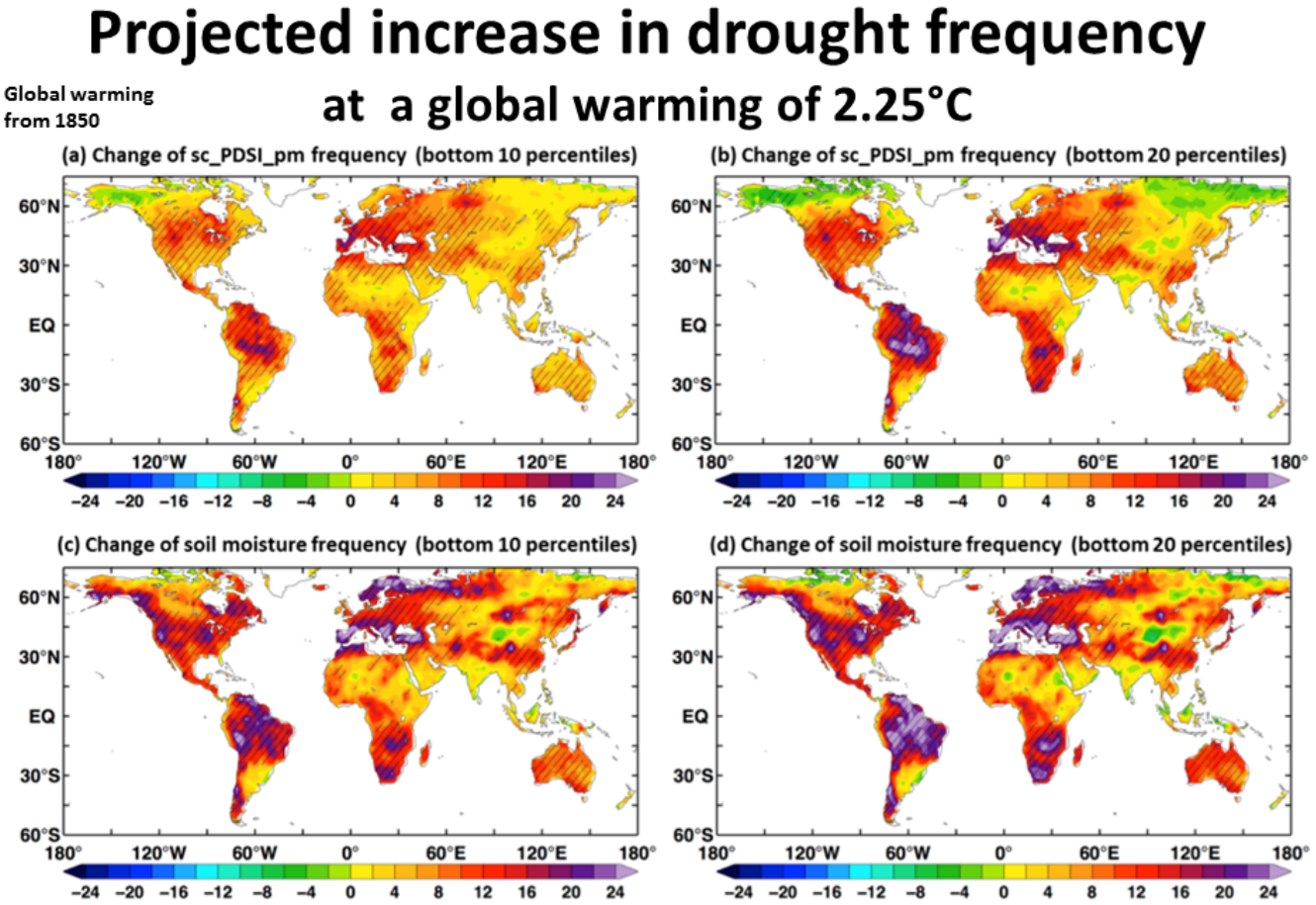


FIG. 8: Multi-model ensemble averaged changes of drought frequency (defined as the percentage of the time in drought conditions, not percentage changes) from 1970–1999 to 2070–2099 under the RCP 4.5 scenario,. The stippling indicates at least 80% of the models agreeing on the sign of change. (From Zhao and Dai 2014)

# IMPLICATIONS OF CLIMATE CHANGE

Precipitation

**Expected Changes**

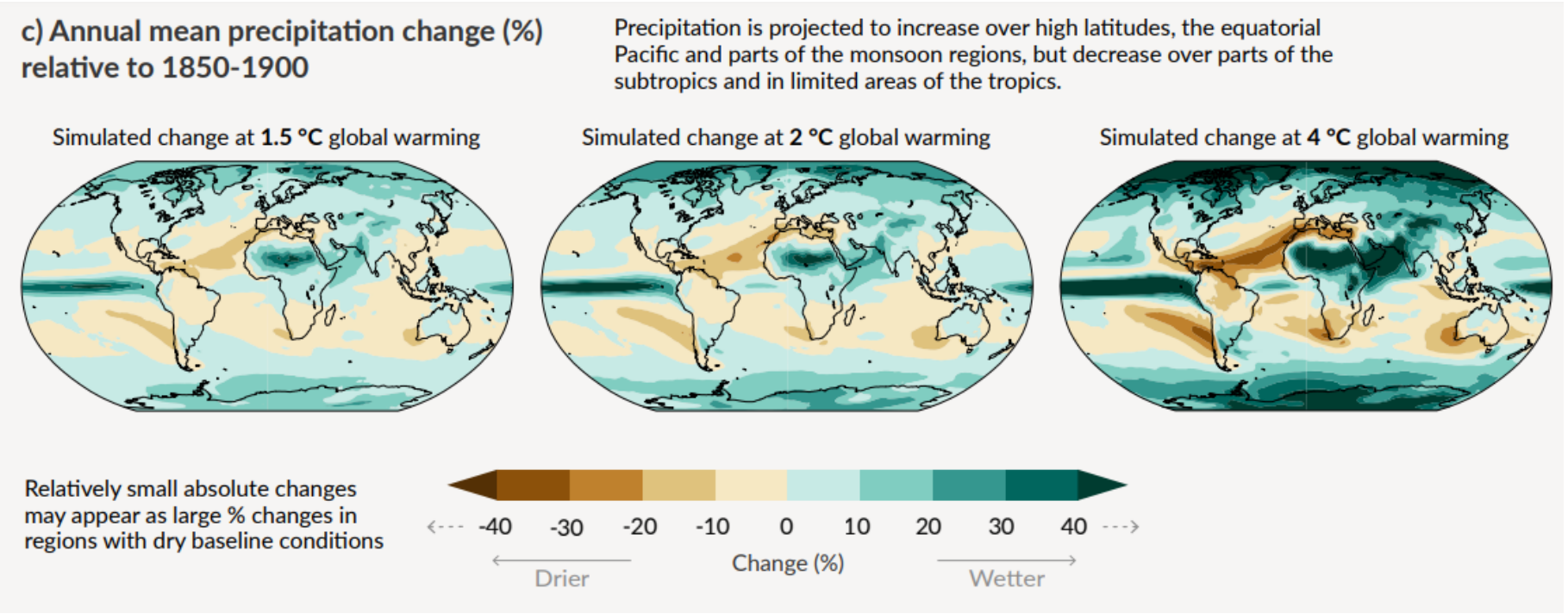


- ✓ **Large increases** in precipitation are expected at **high latitudes** but **also in the equatorial band** as a consequence of an increasing atmospheric convergence of moisture.
- ✓ In contrast, significant **decreases** (of up to 20%) can be expected in the **Mediterranean** region, the **Caribbean** region and more **generally at subtropical** latitudes, including most continental west coasts.

- ✓ On the whole, precipitation **over the land (ocean)** will **increase** slightly by 2100, by **about 5% (4%)** but with large regional asymmetries.
- ✓ It should be noted that increases in precipitation **in high latitudinal bands** are expected to occur **throughout the year**, while increases in more **tropical regions will be restricted to particular seasons** such as JJA for the South Asian Monsoon or DJF for the Australian Monsoon

# Large Scale Circulation projected changes and their effect on the water cycle

## Poleward expansion of Hadley Cells

**Effect:** Broadening of the Hadley Cells and poleward expansion of subtropical dry zones

**Regions:** Uncertain influence on drying of subtropical land regions that are also controlled by evolving surface temperature patterns

**Confidence:** Low

## Poleward migration of storm tracks

Northern hemisphere


**Confidence:** Low

Southern hemisphere


**Confidence:** Medium

**Effect:** Annual-mean mid-latitude storm tracks shifting polewards.

**Regions:** Regional storm tracks moving polewards at different rates in different basins. Southern hemisphere storm tracks have moved polewards more clearly, partly driven by ozone depletion. Poleward movement likely to weaken as ozone hole recovers.

The maps show the effect of 3°C of global warming on mean P-E compared to preindustrial levels (1850-1900)

Annual mean

Seasonal mean

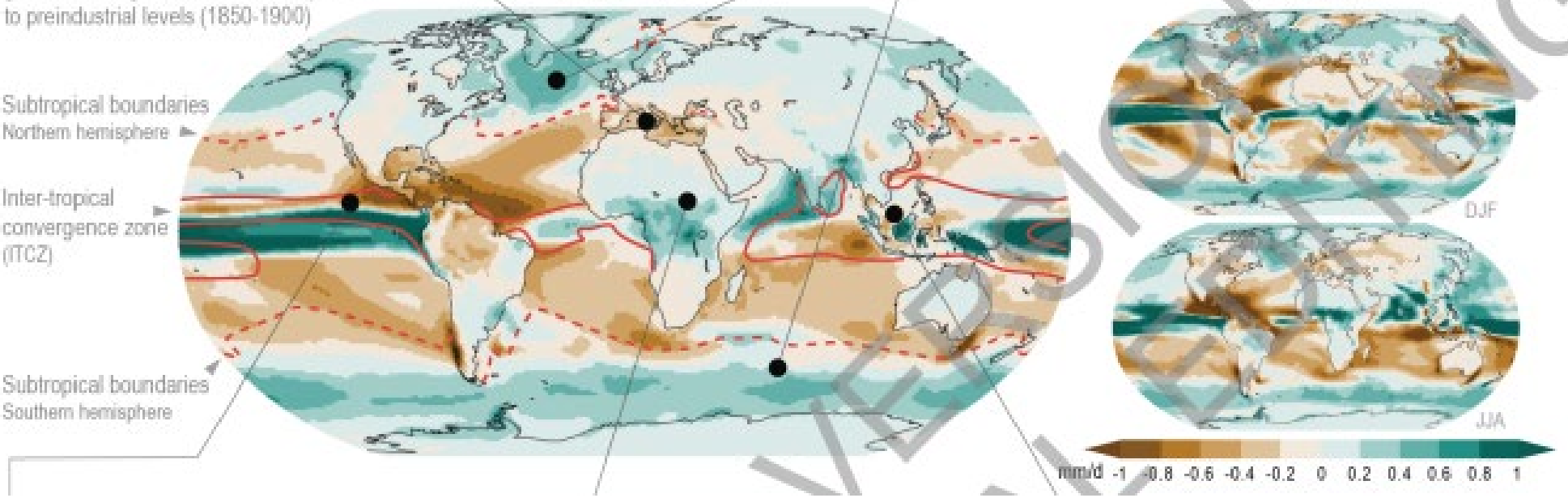




https://www.ipcc.ch/report/ar6/wg1/#FullReport

# IMPLICATIONS OF CLIMATE CHANGE

Expected Changes

## Evaporation

Changes in annual mean evaporation resemble the pattern of changes in temperature, with **increases over most of the ocean**, with a few exceptions such as to the south of Greenland, where decreasing evaporation is matched by decreasing temperature.

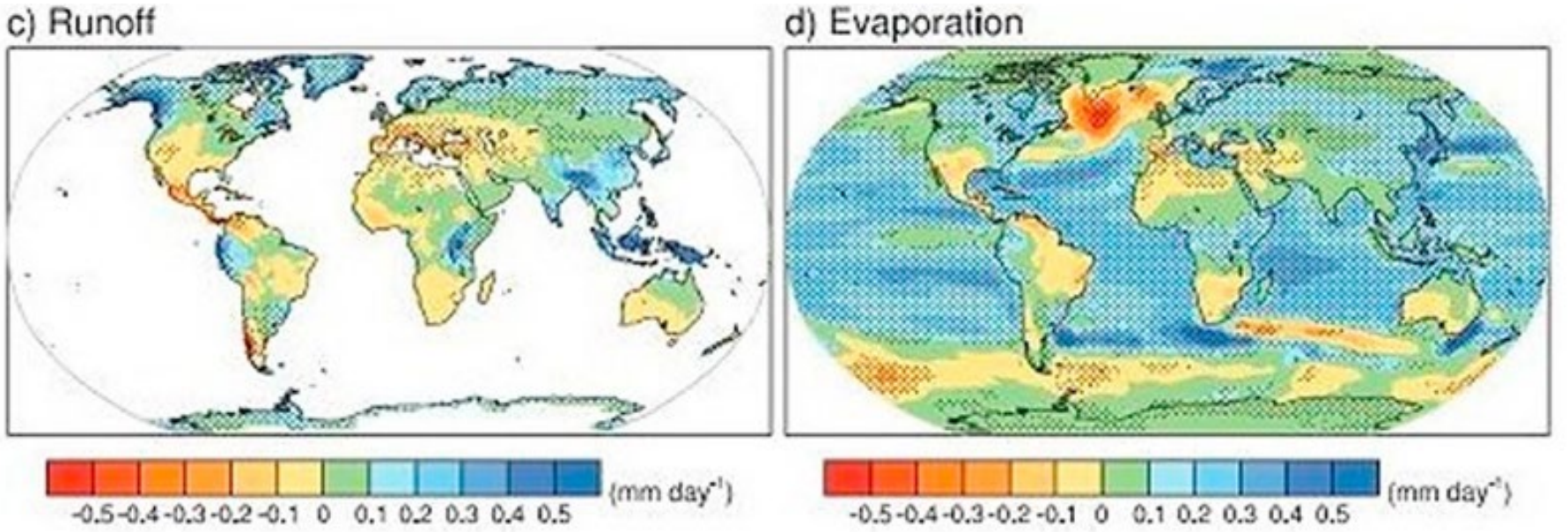


*As in previous figure but for Multimodel mean changes in (c) runoff (mm d–1), and (d) evaporation (mm d–1). Runoff changes are shown at land points with valid data from at least 10 models*

## Runoff

Changes in runoff are bound to **reflect the changes described above in precipitation and evaporation**, being characterized by significant reductions in the Mediterranean basin and Central America but also by **increases in Southeast Asia**, the **African Great Lakes**, and at **high latitudes**

# IMPLICATIONS OF CLIMATE CHANGE

Expected Changes

E-P

- ✓ The general distribution of E-P shows a **poleward expansion of the dry subtropical regions** and wetter middle-to-high latitudes associated with two distinct aspects of global circulation, namely the expansion of the Hadley cell and the poleward shift in the midlatitude storm tracks.

- ✓ Changes in E-P are consequent to these circulation changes, i.e., **the tropics**, along with the middle to high latitudes, **become wetter** (a decrease in E-P), and the **subtropics become drier** (an increase in E-P).

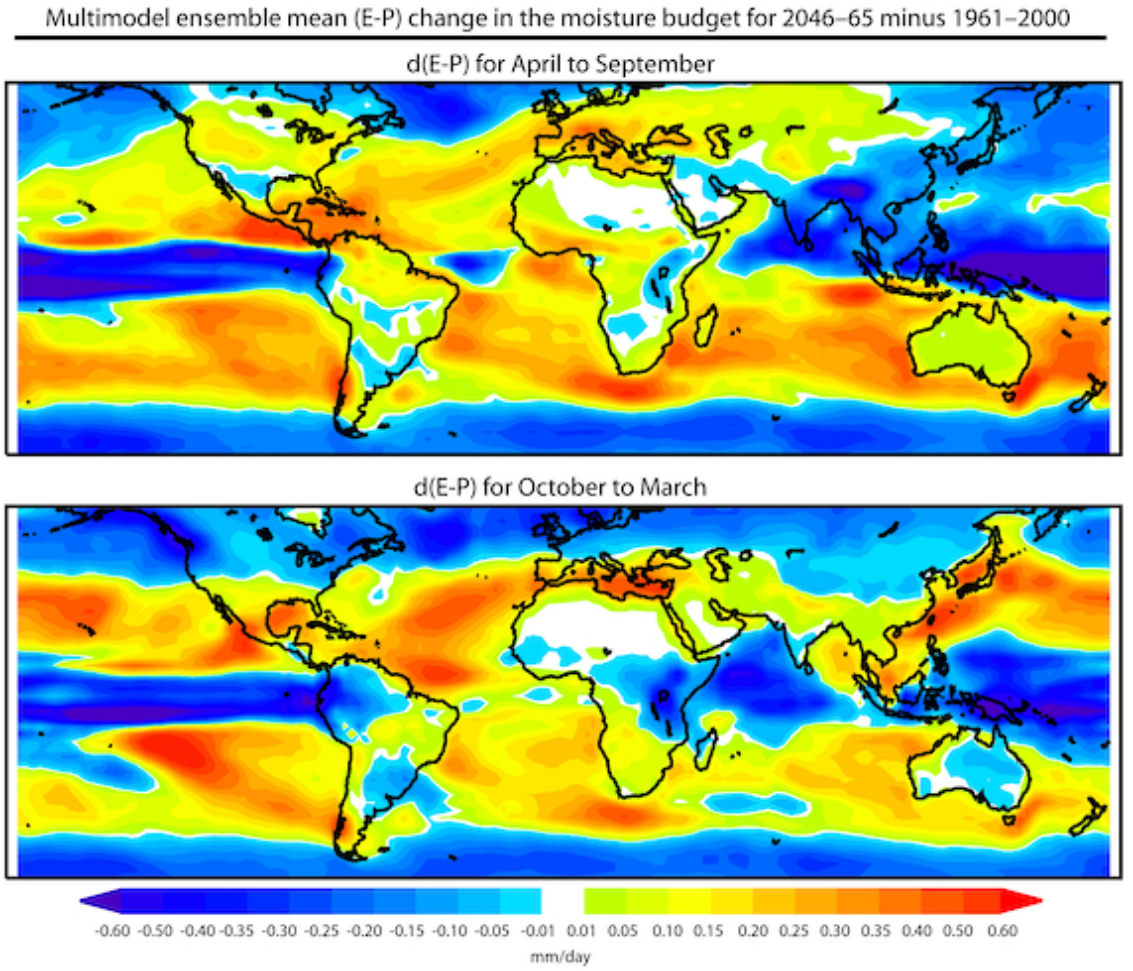


*The climatological multimodel ensemble mean change in the moisture budget for the difference between evaporation and precipitation for (top) April to September and (bottom) October to March 2046–2065, relative to 1961–2000. Units are mm d−1.*

- ✓ This evolution suggests that **the major oceanic sources of moisture** as indicated in previous figures will probably **increase in intensity**, thereby **providing more moisture for precipitation**.
- ✓ These results seem to show how changes in mean circulation appear to cause a decrease in E-P in the equatorial regions between 160 E and 70W. The increase in E-P to the north and south of this band are thought to be related to a shift in the ITCZ

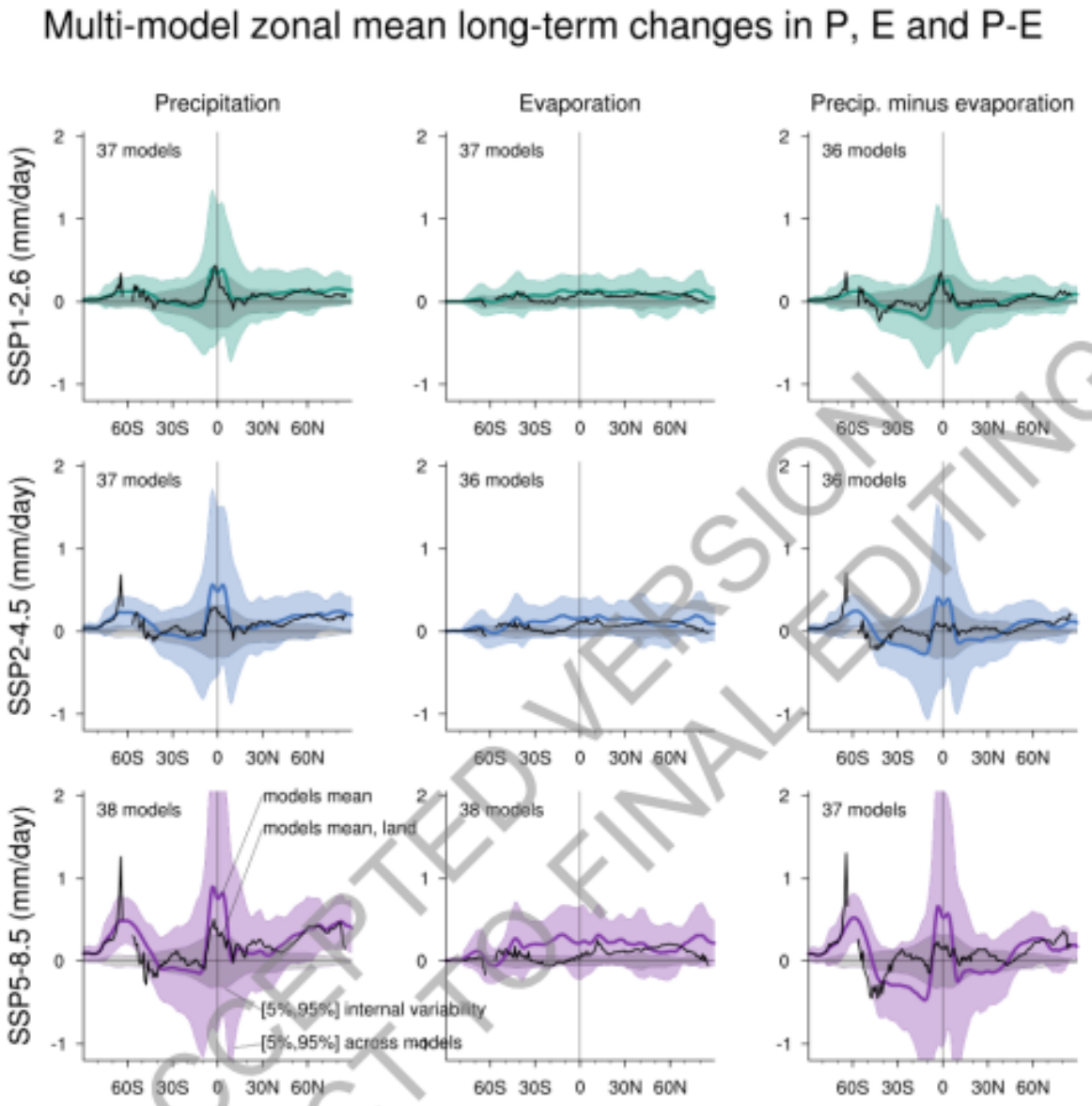


**Figure 8.13: Zonal and annual mean projected long-term changes in the atmospheric water budget.** Zonal and annual mean projected changes (mm/day) in P (precipitation, left column), E (evaporation, middle column), and P-E (right column) over both land and ocean areas (thick line) and over land only (dashed line) averaged across 36 to 38 CMIP6 models in the SSP1-2.6 (a,b), SSP2-4.5 (c,d) and SSP5-8.5 (e,f) scenario, respectively. Shading denotes confidence intervals estimated from the CMIP6 ensemble under a normal distribution hypothesis. Color shading denotes changes over both land and ocean. Grey shading represents internal variability derived from the pre-industrial control simulations. All changes are estimated for 2081-2100 relative to the 1995-2014 base period. Further details on data sources and processing are available in the chapter data table (Table 8.SM.1).

# FUTURE CHALLENGES

A number of questions nevertheless remain within the current scientific state-of-the-art knowledge, namely the following:

(1) Have the moisture source regions been stationary throughout the years, or have they changed location significantly over the last three decades?

(2) How can changes in intensity (more evaporation) and position of the sources affect the distribution of continental precipitation?

(3) What is the role of the main modes of climate variability such as NAO or ENSO in the variability of the moisture source regions?

(4) How much moisture is there, and where is it being transported, by low-level jets and atmospheric rivers and what is the role of these in extreme events?

(5) Do droughts result mainly from a lack of evaporation over the identified main moisture source areas and/or circulation anomalies in the transport?

(6) What is the role of the warm pools (oceanic regions of intense evaporation) in the supply of moisture?

(7) How will climate change alter the location and significance of source regions and the transport of moisture from these toward continental areas in the future?

All these important scientific questions require further study in order to be addressed in depth in future years.